

# Phase-Noise Limitations on Nonlinear-Optical Quantum Computing

by

Justin Dove

B.S., Adelphi University (2012)

Submitted to the Department of Electrical Engineering and Computer  
Science

in partial fulfillment of the requirements for the degree of

Master of Science in Electrical Engineering and Computer Science

at the

MASSACHUSETTS INSTITUTE OF TECHNOLOGY

June 2014

© Massachusetts Institute of Technology 2014. All rights reserved.

Author .....  
Department of Electrical Engineering and Computer Science  
May 19, 2014

Certified by .....  
Jeffrey H. Shapiro  
Julius A. Stratton Professor of Electrical Engineering  
Thesis Supervisor

Accepted by .....  
Leslie A. Kolodziejski  
Chairman, Department Committee on Graduate Theses



# Phase-Noise Limitations on Nonlinear-Optical Quantum Computing

by

Justin Dove

Submitted to the Department of Electrical Engineering and Computer Science  
on May 19, 2014, in partial fulfillment of the  
requirements for the degree of  
Master of Science in Electrical Engineering and Computer Science

## Abstract

Flying in the face of the long-sought-after goal of building optical quantum computers, we show that traditional approaches leveraging nonlinear-optical cross phase modulation (XPM) to construct the critical element, the CPHASE gate—a gate which seeks to impart a  $\pi$ -radian phase shift on a single photon pulse, conditioned on the presence of a second single photon pulse—are doomed to fail. The traditional story told in common textbooks fails to account for the continuous-time nature of the real world. Previous work addressing this fact—finding that the proper continuous-time theory introduces fidelity-degrading phase noise that precludes such proposals—was limited in scope to the case of co-propagating pulses with equal group velocities. This left room for criticism that a high-fidelity CPHASE gate might be constructed using XPM with pulses that pass through each other. In our work, we build such a continuous-time quantum theory of XPM for pulses that pass through each other and evaluate its consequences. We find that fundamental aspects of the real world prevent one from constructing a perfect CPHASE gate, even in theory, and we show that the best we can do seems to fall far short of what is needed for quantum computation, even if we are extremely optimistic.

Thesis Supervisor: Jeffrey H. Shapiro

Title: Julius A. Stratton Professor of Electrical Engineering



## Acknowledgments

I would like to thank the Defense Advanced Research Projects Agency (DARPA) and the National Science Foundation (NSF) for funding this work through their QuEST and IGERT programs, respectively. I would also like to thank my friends and family for their patience, understanding, and support throughout the time it took to complete and document this work. Special thanks is reserved for Chris Chudzicki, whose work provided the foundation of this thesis. Section 2.1 was adapted from his research notes [1], and the derivations in Appendix A were heavily inspired by the same notes. Finally, I wish to express my utmost gratitude to my advisor, Prof. Jeffrey H. Shapiro, without whose insightful guidance and generous assistance this work would not have been possible.



# Contents

<b>1</b>	<b>Introduction</b>	<b>11</b>
1.1	Background . . . . .	11
1.2	Continuous-Time Quantum XPM . . . . .	13
<b>2</b>	<b>XPM with Differing Group Velocities</b>	<b>19</b>
2.1	The Theory . . . . .	19
2.2	Conditions for a Uniform Phase Shift . . . . .	23
<b>3</b>	<b>Fidelity Analysis</b>	<b>27</b>
3.1	The Vacuum Fidelity . . . . .	27
3.2	Response-Independent Results . . . . .	29
3.3	Response-Dependent Results . . . . .	31
<b>4</b>	<b>Principal-Mode Projection</b>	<b>35</b>
4.1	Phase-Noise Injection as a Beam Splitter . . . . .	35
4.2	The Effect of PMP on Fidelity without Cascading . . . . .	39
4.3	Cascading PMP . . . . .	40
<b>5</b>	<b>Conclusions and Future Work</b>	<b>43</b>
<b>A</b>	<b>XPM with Counter-Propagating Pulses</b>	<b>45</b>
A.1	Classical XPM . . . . .	45
A.2	Quantum XPM . . . . .	48
A.3	Conditions for a Uniform Phase Shift . . . . .	54





# List of Figures

1-1	The basic configuration of XPM and the associated field operators. . .	14
2-1	Infinitesimal mismatch and basic XPM media are interleaved to model XPM with differing group velocities. . . . .	20
3-1	A plot of the maximum vacuum fidelity vs. the damping parameter of the single-resonance, two-pole response. . . . .	32
4-1	A beam splitter whose input-output relation is analogous to the phase-noise injection of XPM. . . . .	38
4-2	A train of beam splitters, analogous to the phase-noise behavior of cascading $N$ XPM+PMP elements. . . . .	40



# Chapter 1

## Introduction

### 1.1 Background

Quantum theory seems to have an imperishable impact on all fields it touches, and computation is no exception. The allure of quantum computation is unavoidable. On the one hand, the ability to break RSA cryptosystems [2] is an extremely enticing prospect to those in the defense and security communities. Meanwhile, fundamental speedups in search algorithms [3], certain problems involving linear systems [4], machine learning, and yet other computational problems yield much to desire for the computation industry at large. Beyond this, the ability to efficiently simulate quantum systems [5] seems to promise vast advances in quantum chemistry and subsequently medicine. So, it seems safe to say that many people from many fields can agree that universal quantum computers are a technology worth pursuing.

Within the field of quantum computation, one of the largest open questions is that of what architecture to use; that is, how to physically construct such devices, what physical systems to map the theory onto. Although each physical system has its fair share of benefits and drawbacks, optics stands out as a particularly exciting candidate for quantum computation research. In short, optics is a relatively nice framework to work in experimentally and has a long history of being useful in studying quantum phenomena. This can largely be attributed to the fact that the tools necessary to do quantum computation in optics, or explore most any quantum phe-

nomena for that matter, are tools that are strongly sought after outside of the field and are thus the focus of their own research independently. Single-photon sources continue to be improved and are seeking the same ideal necessary for reliable qubit generation. Single-photon detection likewise is being vigorously pursued and being optimized, incidentally or not, for qubit measurement. Meanwhile, single-qubit control is already quite robustly achievable thanks to years of work in interferometry. As it stands, optics is already a crucial framework for classical communication and even a continuing area of much research for classical computation. So, it is natural to pursue quantum computation in this setting.

But despite its remarkable pedigree and natural fluency in all things quantum, optics is not without an Achilles' heel. It has proved extremely challenging to develop high-fidelity, deterministic, two-qubit entangling gates, such as the CPHASE gate. One of the most notable developments in this direction was the work of Knill, Laflamme, and Milburn [6], which proposed an all-linear-optical solution to this problem. While their scheme for quantum computation is attractive on account of only using linear optics, the difficulty is traded off by its reliance on high-efficiency adaptive measurement techniques and large quantities of ancilla photons, leaving the scheme still out of reach for current technology. So, it remains prudent to continue research on more traditional approaches to the two-qubit-gate problem, namely the nonlinear-optical approach suggested by Chuang and Yamamoto [7].

The nonlinear-optical approach to generating a two-photon entangling gate, specifically the CPHASE gate, relies on using the cross-Kerr effect to impart a  $\pi$  phase shift on one single-photon pulse conditioned on the presence of another. Modeling this interaction by the two-mode Hamiltonian

$$H_{\text{XPM}} = -\chi \hat{a}^\dagger \hat{a} \hat{b}^\dagger \hat{b}, \quad (1.1)$$

where  $\hat{a}$  and  $\hat{b}$  are the photon-annihilation operators for the two modes, and  $\chi$  characterizes the nonlinearity of the interaction material, one can show that the desired behavior is attainable, as demonstrated by Chuang and Yamamoto. The catch how-

ever, is that attaining this behavior requires an exceedingly strong nonlinearity, far beyond that of the materials we have found or developed to date. So, the problem seems to reduce to one of materials science.

That said, an astute reader will note that the Hamiltonian presented in Equation (1.1) is overly simplistic: it models each of the two spatial optical modes as single quantum harmonic oscillators. We know that a complete theory of quantum optics must account for all frequencies of the electromagnetic field, treating each as an independent mode. It stands to reason then that this traditional approach to using cross-phase modulation (XPM) must be reanalyzed in a full, multimode, continuous-time treatment. XPM itself was lacking a multimode, continuous-time quantum theory until relatively recently when one was developed by Shapiro and Bondurant [8], which extended earlier work on the multimode, continuous-time quantum theory of self-phase modulation (SPM) by Boivin et al. [9]. Their theory can be summarized as follows.

## 1.2 Continuous-Time Quantum XPM

As with standard quantized electromagnetism, a positive-frequency, photon-units field operator, analogous to the annihilation operator of the simple harmonic oscillator, is associated with each polarization of every spatial mode. Limiting our consideration to nonlinear optics in single spatial-mode scenarios, such as fiber, and taking each of our two interacting fields to only have a single excited polarization, in the context of XPM we are concerned with four such operators:  $\hat{E}_A^{\text{in}}(t)$ , the field-operator for the first spatial mode of the input facet of the nonlinear material,  $\hat{E}_B^{\text{in}}(t)$ , the field-operator for the second spatial mode at that input facet, and  $\hat{E}_A^{\text{out}}(t)$  and  $\hat{E}_B^{\text{out}}(t)$ , the corresponding operators at the nonlinear material's output facet, as shown in Figure 1-1. The output field operators are defined in such a way so as to suppress the group delay associated with the pulses propagating through the XPM material.

We appeal to the Heisenberg-picture to describe the spatial-evolution of the operator for each mode by an operator input-output relation, which in this case is given



Figure 1-1: The basic configuration of XPM and the associated field operators.

by:

$$\hat{E}_A^{\text{out}}(t) = e^{i\hat{\xi}_A(t)} e^{i\hat{\zeta}_A(t)} \hat{E}_A^{\text{in}}(t) \quad (1.2a)$$

$$\hat{E}_B^{\text{out}}(t) = e^{i\hat{\xi}_B(t)} e^{i\hat{\zeta}_B(t)} \hat{E}_B^{\text{in}}(t). \quad (1.2b)$$

Here, the  $\hat{\zeta}(t)$  operators are the *phase-shift* operators responsible for imparting the cross-phase modulation on each mode and are given by:

$$\hat{\zeta}_A(t) = \kappa \int ds \, h(t-s) \, \hat{I}_B^{\text{in}}(s) \quad (1.3a)$$

$$\hat{\zeta}_B(t) = \kappa \int ds \, h(t-s) \, \hat{I}_A^{\text{in}}(s), \quad (1.3b)$$

where  $\kappa$  is the XPM coupling coefficient,  $h(t)$  is the normalized ( $\int dt \, h(t) = 1$ ) XPM response function of the material, and  $\hat{I}(t) = \hat{E}^\dagger(t)\hat{E}(t)$  is the photon-flux operator. Note, since the  $\hat{\zeta}(t)$  and  $\hat{\xi}(t)$  operators are Hermitian, we have  $\hat{I}^{\text{in}}(t) = \hat{I}^{\text{out}}(t)$  for both fields. Also note, the phase-shift operator for each mode is related to the photon-flux operator for the *other* mode. Meanwhile, the  $\hat{\xi}(t)$  operators are the *phase-noise* operators. The introduction of these operators arises out of the need to preserve the standard free-field commutation relation,

$$[\hat{E}(t), \hat{E}^\dagger(s)] = \delta(t-s), \quad (1.4)$$

for each spatial mode. These operators are defined in terms of separate, auxiliary field operators  $\hat{B}(\omega)$  and  $\hat{C}(\omega)$  that are introduced as a model for the XPM material

itself:

$$\hat{\xi}_A(t) \equiv \int_0^\infty \frac{d\omega}{2\pi} \sqrt{\kappa H_{\text{im}}(\omega)} \{[\hat{B}(\omega) - i\hat{C}^\dagger(\omega)]e^{-i\omega t} + \text{hc}\}, \quad (1.5a)$$

$$\hat{\xi}_B(t) \equiv \int_0^\infty \frac{d\omega}{2\pi} \sqrt{\kappa H_{\text{im}}(\omega)} \{[\hat{B}(\omega) + i\hat{C}^\dagger(\omega)]e^{-i\omega t} + \text{hc}\}. \quad (1.5b)$$

Here  $H_{\text{im}}(\omega)$  is the imaginary part of  $H(\omega) = \int dt h(t)e^{i\omega t}$ , the Fourier transform of  $h(t)$ ,  $\kappa$  characterizes the strength of the nonlinearity, and hc represents the Hermitian conjugate of the preceding term. The resulting noise is understood to be a phenomenological model for the noise induced by Raman scattering, which has been experimentally observed in fiber by Voss and Kumar [10]. The fine details of these operators are not of great importance. Instead, it suffices to note that they are characterized by the commutation relations

$$[\hat{\xi}_A(t), \hat{\xi}_A(s)] = [\hat{\xi}_A(t), \hat{\xi}_A(s)] = 0 \quad (1.6a)$$

$$[\hat{\xi}_A(t), \hat{\xi}_B(s)] = i\kappa[h(s-t) - h(t-s)], \quad (1.6b)$$

and that, taking  $\hat{B}(\omega)$  and  $\hat{C}(\omega)$  to be in thermal states with temperature  $T$ , they are in a zero-mean jointly Gaussian state with symmetrized autocorrelation functions

$$\langle\{\hat{\xi}_A(t), \hat{\xi}_A(s)\}\rangle = \langle\{\hat{\xi}_A(t), \hat{\xi}_A(s)\}\rangle = \int \frac{d\omega}{\pi} S_{\xi\xi}(\omega) \cos[\omega(t-s)], \quad (1.7)$$

with spectrum

$$S_{\xi\xi}(\omega) = \kappa H_{\text{im}}(\omega) \coth\left(\frac{\hbar\omega}{2k_B T}\right), \quad (1.8)$$

where  $\hbar$  is the reduced Planck constant, and  $k_B$  is the Boltzmann constant. For the theory to make physical sense, it must be the case that  $\forall \omega \geq 0 : H_{\text{im}}(\omega) \geq 0$  [9, 11].

In this framework, Shapiro [12] went on to analyze the operation of a CPHASE gate in which two pulses co-propagate in an XPM material. First, he noted that in order to agree with established classical results, the response function cannot be instantaneous. Furthermore, it obviously must be restricted to be causal. In the fast-response regime, in which the duration of the response function is much shorter

than the duration of the qubit-carrying temporal modes (pulses) of  $\hat{E}_A^{\text{in}}(t)$  and  $\hat{E}_B^{\text{in}}(t)$ , Shapiro found that it was impossible to achieve a uniform phase shift over the entire target pulse. Heuristically, this can be explained by the presence of the photon-flux operator in Equation (1.3); for example, postselected on the detection of a photon in field  $A$ , the phase shift on the field- $B$  pulse only exists at a very localized position. In the slow-response regime, in which the response function's duration greatly exceeds that of the pulses, and assuming the two-pole frequency response function

$$H(\omega) = \frac{\omega_0^2}{\omega_0^2 - \omega^2 - i\omega\gamma}, \quad (1.9)$$

where  $\omega_0$  is the resonant frequency and  $\gamma$  is the damping factor, Shapiro found that the phase noise prevented high-fidelity operation of the gate, even at  $T = 0$  K. Moreover, to achieve a uniform phase shift with a slow-response, *causal* response function, one must delay the target pulse, breaking the control/target symmetry that is critical for a proper CPHASE gate. In short, the target will be unable to induce a phase-shift on the control.

The analysis presented by Shapiro leaves open the following nagging question: what if one pulse propagates *through* the other in a fast-response material? It would seem that this should alleviate the issues with the non-uniformity of fast-response phase shifts by dragging the localized phase shift through the target, so to speak. Indeed, this technique has had success in classical switching in fiber and behaves as expected. Moreover, several researchers [13–16] have suggested applying this technique to the quantum case. The question, however, is whether or not this technique will also result in dragging excessive phase noise through the pulses, degrading the fidelity beyond usefulness. This question will be answered in this thesis.

This thesis is organized as follows. Having summarized the relevant background information in this chapter, Chapter 2 will be devoted to developing a continuous-time quantum theory of XPM for pulses with differing group velocities. (Appendix A offers a parallel development for XPM with counter-propagating pulses.) Chapter 3 will use this theory to analyze the fidelity of the CPHASE gate. Chapter 4 will then extend



the analysis of Chapter 3 to consider a recently-developed form of error correction for such systems. Finally, Chapter 5 will be dedicated to summarizing the results and offering options for future research.



## Chapter 2

# XPM with Differing Group Velocities

While the continuous-time quantum theory of XPM described in Chapter 1 does succeed at addressing the flaw in the traditional single-mode analysis of the nonlinear-optical CPHASE gate, it has at its core, baked in, the assumption that the single-photon pulses in each of the two fields propagate with the same group velocity. So, it is impossible to analyze the case where one pulse propagates through the other using this theory. Instead, we must build a new continuous-time quantum theory of XPM with differing group velocities.

### 2.1 The Theory

We can develop such a theory by modeling the XPM material as an alternating pattern of two types of materials: *mismatch* media in which the group velocities of the two fields differ, but no XPM interaction takes place; and *basic XPM* media in which the XPM interaction takes place, but the group velocities of the two fields are the same, as shown in Figure 2-1. In the limit that the each XPM+mismatch medium is infinitesimally thick and the number  $N$  of XPM+mismatch cascades approaches infinity so that the overall thickness of the cascade stays constant, we obtain an XPM theory for differing group velocities.

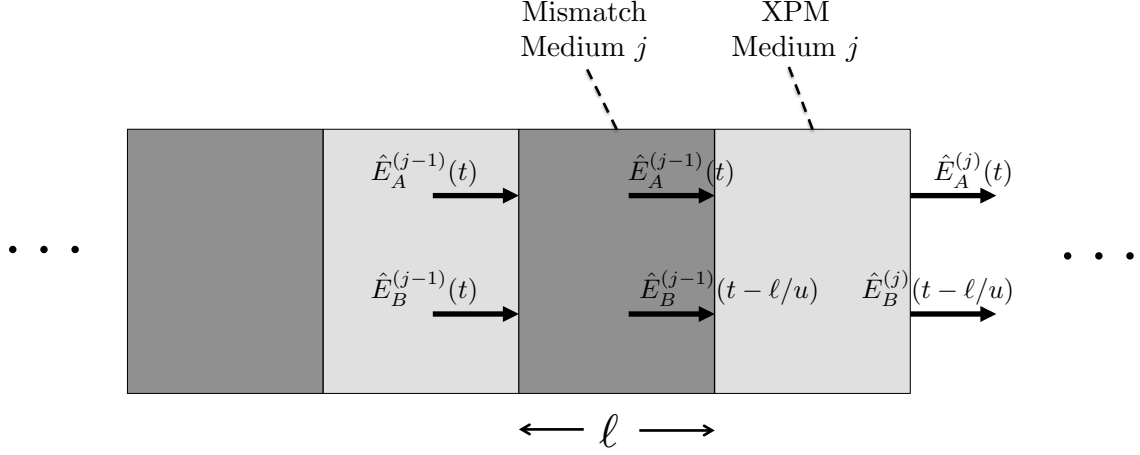


Figure 2-1: Infinitesimal mismatch and basic XPM media are interleaved to model XPM with differing group velocities.

Each medium is of length  $\ell$ , each basic XPM medium has strength  $\frac{\kappa}{N} = \eta\ell$ , and in the mismatch media  $1/u = 1/v_A - 1/v_B$  where  $v_A$  and  $v_B$  are the group velocities of fields  $A$  and  $B$  respectively. We have in mind that in these mismatch media  $v_B > v_A$  so that pulse  $B$  can overtake pulse  $A$ . Let  $\hat{E}_K^{(j)}(t)$  denote field  $K$  (where  $K \in \{A, B\}$ ) at the output of the  $j^{\text{th}}$  XPM medium, and  $\hat{I}_K^{(j)}(t)$  denote the corresponding intensity. Then:

$$\hat{E}_A^{(j)}(t) = \exp[\mathrm{i}\hat{\xi}_A^{(j)}(t)] \exp\left[\mathrm{i}\eta\ell \int \mathrm{d}t' h(t-t') I_B^{(j-1)}(t' - \ell/u)\right] \hat{E}_A^{(j-1)}(t), \quad (2.1a)$$

$$\hat{E}_B^{(j)}(t - \ell/u) = \exp[\mathrm{i}\hat{\xi}_B^{(j)}(t - \ell/u)] \exp\left[\mathrm{i}\eta\ell \int \mathrm{d}t' h(t - \ell/u - t') I_A^{(j-1)}(t')\right] \hat{E}_B^{(j-1)}(t), \quad (2.1b)$$

and

$$\hat{I}_A^{(j)}(t) = \hat{I}_A^{(j-1)}(t), \quad (2.2a)$$

$$\hat{I}_B^{(j)}(t) = \hat{I}_B^{(j-1)}(t + \ell/u). \quad (2.2b)$$

Here the  $\hat{\xi}_K^{(j)}$ s are independent for different  $j$ . Since the  $A$  field maintains the same group velocity throughout the entire process, but the  $B$  field speeds up in the mismatch media, we have that the  $\hat{I}_A^{(j)}(t) = \hat{I}_A^{(0)}(t)$ , while  $\hat{I}_B^{(j)}(t) = \hat{I}_B^{(0)}(t + j\ell/u)$ .

Our goal is to relate the input fields  $\hat{E}_A^{\text{in}}(t) \equiv \hat{E}_A^{(0)}(t)$  and  $\hat{E}_B^{\text{in}}(t) \equiv \hat{E}_B^{(0)}(t)$  to the output fields

$$\hat{E}_A^{\text{out}}(t) \equiv \hat{E}_A^{(N)}(t), \quad (2.3a)$$

$$\hat{E}_B^{\text{out}}(t) \equiv \hat{E}_B^{(N)}(t - N\ell/u). \quad (2.3b)$$

The output  $A$  field is not so bad, it is:

$$\hat{E}_A^{\text{out}}(t) = \exp \left[ i \sum_{j=1}^N \hat{\xi}_A^{(j)}(t) \right] \exp \left[ i \sum_{j=1}^N \hat{\zeta}_A^{(j)}(t) \right] \hat{E}_A^{\text{in}}(t), \quad (2.4)$$

with

$$\begin{aligned} \sum_{j=1}^N \hat{\zeta}_A^{(j)}(t) &= \eta \sum_{j=1}^N \ell \int dt' h(t-t') I_B^{(j-1)}(t - \ell/u) \\ &= \eta \sum_{j=1}^N \ell \int dt' h(t-t') \hat{I}_B^{\text{in}}(t + j\ell/u - 2\ell/u). \end{aligned} \quad (2.5)$$

The output of field  $B$  is a bit trickier:

$$\begin{aligned} \hat{E}_B^{(N)}(t - N\ell/u) &= \exp \left[ i \hat{\xi}_B^{(N)}(t - N\ell/u) \right] \exp \left[ i \eta \ell \int dt' h(t - N\ell/u - t') \hat{I}_A^{\text{in}}(t') \right] \\ &\quad \times \hat{E}_B^{(N-1)}\left(t - \frac{N-1}{u}\ell\right) \\ &= \exp \left[ i \hat{\xi}_B^{(N)}(t - N\ell/u) \right] \exp \left[ i \eta \ell \int dt' h(t - N\ell/u - t') \hat{I}_A^{\text{in}}(t') \right] \\ &\quad \times \exp \left[ i \hat{\xi}_B^{(N-1)}\left(t - \frac{N-1}{u}\ell\right) \right] \exp \left[ i \eta \ell \int dt' h\left(t - \frac{N-1}{u}\ell - t'\right) \hat{I}_A^{\text{in}}(t') \right] \\ &\quad \times \hat{E}_B^{(N-2)}\left(t - \frac{N-2}{u}\ell\right) \\ &\quad \vdots \\ &= \exp \left[ i \sum_{j=1}^N \hat{\xi}_A^{(j)}(t - j\ell/u) \right] \exp \left[ i \sum_{j=1}^N \hat{\zeta}_B^{(j)}(t) \right] \hat{E}_B^{\text{in}}(t), \end{aligned} \quad (2.6)$$

where

$$\begin{aligned}\sum_{j=1}^N \zeta_B^{(j)}(t) &= \eta \sum_{j=1}^N \ell \int dt' h(t - j\ell/u - t') \hat{I}_A^{\text{in}}(t') \\ &= \eta \sum_{j=1}^N \ell \int dt'' h(t - t'') \hat{I}_A^{\text{in}}(t'' - j\ell/u).\end{aligned}\quad (2.7)$$

In the  $N \rightarrow \infty$ ,  $\ell \rightarrow 0$ ,  $N\ell = L$  limit, we obtain

$$\hat{E}_A^{\text{out}}(t) = e^{i\hat{\xi}_A(t)} e^{i\hat{\zeta}_A(t)} \hat{E}_A^{\text{in}}(t), \quad (2.8a)$$

$$\hat{E}_B^{\text{out}}(t) = e^{i\hat{\xi}_B(t)} e^{i\hat{\zeta}_B(t)} \hat{E}_B^{\text{in}}(t), \quad (2.8b)$$

where

$$\hat{\zeta}_A(t) = \eta \int_0^L dz \int ds h(t - s) \hat{I}_B^{\text{in}}(s + z/u), \quad (2.9a)$$

$$\hat{\zeta}_B(t) = \eta \int_0^L dz \int ds h(t - s) \hat{I}_A^{\text{in}}(s - z/u), \quad (2.9b)$$

and

$$\hat{\xi}_A(t) = \lim_{N \rightarrow \infty, N\ell=L} \sum_{j=1}^N \hat{\xi}_A^{(j)}(t) \quad (2.10a)$$

$$\hat{\xi}_B(t) = \lim_{N \rightarrow \infty, N\ell=L} \sum_{j=1}^N \hat{\xi}_B^{(j)}(t - j\ell/u) \quad (2.10b)$$

Equation (2.10) is a formal definition of  $\hat{\xi}_A(t)$  and  $\hat{\xi}_B(t)$ , and is not particularly useful. However, we will be assuming that the auxiliary modes defining the  $\hat{\xi}$ s are in a zero-mean Gaussian state, so all we need to know is the commutator  $[\hat{\xi}_K(t), \hat{\xi}_L(s)]$  and the symmetrized autocorrelation function  $\langle \{\hat{\xi}_K(t), \hat{\xi}_K(s)\} \rangle$ . We now turn to working out nice forms for these in the  $N \rightarrow \infty$ ,  $N\ell = L$  limit. We have

$$\begin{aligned}[\hat{\xi}_A(t), \hat{\xi}_B(s)] &= \lim_{N \rightarrow \infty, N\ell=L} \sum_{j=1}^N [\hat{\xi}_A^{(j)}(t), \hat{\xi}_B^{(j)}(s - j\ell/u)] \\ &= \lim_{N \rightarrow \infty, N\ell=L} i\eta \sum_{j=1}^N \ell [h(s - j\ell/u - t) - h(t - s + j\ell/u)] \\ &= i\eta \int_0^L dz [h(s - t - z/u) - h(t - s + z/u)].\end{aligned}\quad (2.11)$$

While the commutator is more complicated than in the original ( $v_A = v_B$ ) theory, the autocorrelation functions  $\langle \{\hat{\xi}_A(t), \hat{\xi}_A(s)\} \rangle$  and  $\langle \{\hat{\xi}_B(t), \hat{\xi}_B(s)\} \rangle$  are seen not to change by linearity and the independence of the separate basic XPM media. That is, these are still given by Equation (1.7) with  $\kappa = \eta L$ .

## 2.2 Conditions for a Uniform Phase Shift

To build a CPHASE gate, each field must receive a uniform  $\pi$ -radian phase shift, with high fidelity, conditioned on the presence of a photon in the other field. Sufficient conditions for ensuring a uniform  $\pi$ -radian phase shift are intuitive and not hard to derive. Keeping in mind that we are working in the Heisenberg picture, for each mode we take the computational basis state  $|0\rangle$  to be the vacuum state, and we take the computational basis state  $|1\rangle$  to be given by

$$|1\rangle = \int_{-\infty}^{\infty} dt \, \psi(t) |t\rangle. \quad (2.12)$$

Here,  $\psi(t)$  is some fixed pulse shape (whose squared magnitude integrates to 1), which, in the interest of the symmetry necessary for quantum computation, we take to be the same shape for both fields (differing at most by a temporal delay) and  $|t\rangle$  is the state of the field in which there is a single photon at time  $t$  and none at all other times. Ignoring the phase noise for the time being, the phase shifts induced on each field by the presence of a single-photon pulse in the other field are found by taking the partial trace of the phase-shift operator for the field with respect to the other field, as follows:

$${}_B\langle 1 | e^{i\hat{\zeta}_A(t)} | 1 \rangle_B = \int ds \, e^{i\eta \int_0^L dz \, h(t-s+z/u)} |\psi_B(s)|^2, \quad (2.13a)$$

$${}_A\langle 1 | e^{i\hat{\zeta}_B(t)} | 1 \rangle_A = \int ds \, e^{i\eta \int_0^L dz \, h(t-s-z/u)} |\psi_A(s)|^2, \quad (2.13b)$$

where a step or two have been omitted. From this, it is clear that a sufficient condition for a uniform phase shift is that the response-function integrals encapsulate

the entirety of the response function for all times  $t$  and  $s$  for which the pulses are non-zero. So, take  $h$  to be non-zero only over the interval  $[0, t_h]$ , ensuring the response is causal, take  $\psi_A$  to be non-zero only over the interval  $[-t_\psi/2, t_\psi/2]$ , so that  $t_\psi$  is the pulse width, and take  $\psi_B$  to be non-zero only over the interval  $[-t_\psi/2 + t_d, t_\psi/2 + t_d]$ , where  $t_d$  represents the temporal delay between pulse  $A$  and pulse  $B$  at the input. While these support conditions may not be able to be met exactly, particularly when the response function and/or pulse shape do not have bounded support, we can at least take  $t_h$  and  $t_\psi$  to represent the nominal durations over which each function is significantly different from zero. Extracting the response-function integrals, and making a small change of variables, the quantities of interest are

$$\phi_A(t, s) = \eta u \int_0^{L/u} dz' h(t - s + z'), \quad (2.14a)$$

$$\phi_B(t, s) = \eta u \int_0^{L/u} dz' h(t - s - z'). \quad (2.14b)$$

For the response function integrals to encapsulate the entirety of the response, it is clear that the following inequalities must hold:

$$t \in \left[-\frac{t_\psi}{2}, \frac{t_\psi}{2}\right], s \in \left[-\frac{t_\psi}{2} + t_d, \frac{t_\psi}{2} + t_d\right] \quad \min_{z' \in [0, \frac{L}{u}]} \{t - s + z'\} \leq 0, \quad (2.15a)$$

$$t \in \left[-\frac{t_\psi}{2}, \frac{t_\psi}{2}\right], s \in \left[-\frac{t_\psi}{2} + t_d, \frac{t_\psi}{2} + t_d\right] \quad \max_{z' \in [0, \frac{L}{u}]} \{t - s + z'\} \geq t_h, \quad (2.15b)$$

$$t \in \left[-\frac{t_\psi}{2} + t_d, \frac{t_\psi}{2} + t_d\right], s \in \left[-\frac{t_\psi}{2}, \frac{t_\psi}{2}\right] \quad \min_{z' \in [0, \frac{L}{u}]} \{t - s - z'\} \leq 0, \quad (2.15c)$$

$$t \in \left[-\frac{t_\psi}{2} + t_d, \frac{t_\psi}{2} + t_d\right], s \in \left[-\frac{t_\psi}{2}, \frac{t_\psi}{2}\right] \quad \max_{z' \in [0, \frac{L}{u}]} \{t - s - z'\} \geq t_h. \quad (2.15d)$$

Plugging in the appropriate maximum and minimum values of  $t$ ,  $s$ , and  $z'$  and removing redundancies results in the following pair of sufficient conditions:

$$t_d \geq t_\psi + t_h \quad (2.16a)$$

$$\frac{L}{u} \geq t_\psi + t_h + t_d. \quad (2.16b)$$



Physically, these conditions make sense. The first condition mandates that pulse  $B$  not enter the material until pulse  $A$  and the entirety of its response tail are completely in the material. The second condition, then, mandates that the material be long enough to allow the entirety of pulse  $B$  and its response tail to overtake pulse  $A$  within the material.

Taking both the delay and the nonlinear material to be as short as possible, we have

$$t_d = t_\psi + t_h \tag{2.17a}$$

$$\frac{L}{u} = 2(t_\psi + t_h). \tag{2.17b}$$

Recalling that the response function is normalized, we see that the magnitude of the uniform phase-shift is given by

$$\phi = \eta u. \tag{2.18}$$

From these facts, we have the following, which will prove useful in Chapter 3,

$$\eta L = 2\phi(t_\psi + t_h). \tag{2.19}$$

Note, the conditions presented here have only been shown to be sufficient for a uniform phase shift, not necessary. One might imagine attaining a uniform phase shift in a way that doesn't involve exposing each point of each pulse to the full duration of the XPM response. However, doing so is notably subtle. Given the architecture of one pulse passing through another, it seems that if not all of each pulse is exposed to the entirety of the response, different portions of that pulse will be exposed to different durations of the response. So, attaining a uniform phase shift in this way, if at all possible, seems to require aggressive engineering of the response function, which seems utterly unlikely to be practically achievable given that we already cannot drive the strength of an XPM nonlinearity to values commensurate with single-photon sensitivity. Consequently we will assume the aforementioned conditions as *the* conditions

for a uniform phase shift for the remainder of the thesis.

As a final note, one might imagine constructing a CPHASE gate by using counter-propagating pulses, approaching each other head on with the same group velocity, as opposed to the co-propagating, differing-group-velocity case presented here. This notably has better symmetry properties, and would thus avoid certain synchronization issues when used in a large circuit. This nicety aside, the strength of the nonlinear material would need to be much higher for counter-propagating pulses, due to the great speed at which they will fly by each other. Nevertheless, it is worth examining this case. So, a continuous-time quantum theory of XPM with counter-propagating, equal-group-velocity pulses is presented in Appendix A. As it turns out, it makes the same critical predictions as the theory presented in this chapter. So, the remainder of this document applies equally well to either case.

# Chapter 3

## Fidelity Analysis

### 3.1 The Vacuum Fidelity

With the question of attaining a uniform phase shift settled, we can now turn our attention to the fidelity of such operations. The most general fidelity we can evaluate would involve measuring the overlap between the actual two-field output state from the XPM interaction and the two-field output state from an ideal CPHASE gate, averaged over arbitrary values of the two-field input state. However, for now, it will suffice for us to examine what we will call the *vacuum fidelity*, introduced by Shapiro [12]. That is, we will assume one of the fields, let's say field  $B$ , is in the vacuum state. Now, assuming our uniform-phase-shift conditions are met, the vacuum fidelity is the overlap between the actual output state and the CPHASE-gate output state of field  $A$ , averaged over all choices of its input state on the Bloch sphere. Moreover, because the  $B$  field is in its vacuum state, the CPHASE-gate output state for field  $A$  is its input state.

In a sense, the vacuum fidelity is the most naive performance metric we can calculate; it corresponds to the fidelity of doing nothing, that is, no interaction between the fields. Clearly it must be high if we are to hope for high fidelity operation at all.

The preceding language of input and output *states* implicitly refers to the Schrödinger picture. So, we'll need to invert our Heisenberg-picture operator input-output relation and solve for the Schrödinger evolution of the field- $A$  state. Assuming field  $B$  is

in vacuum, we have

$$\hat{E}_A^{\text{out}}(t) = e^{i\hat{\xi}_A(t)} \hat{E}_A^{\text{in}}(t). \quad (3.1)$$

Inverting this relation and taking the conjugate transpose, we have

$$\hat{E}_A^{\text{in}\dagger}(t) = e^{i\hat{\xi}_A(t)} \hat{E}_A^{\text{out}\dagger}(t). \quad (3.2)$$

Note that the phase-noise operator  $\hat{\xi}_A(t)$  operates on the auxiliary modes representing the material, not on the state of fields  $A$  and  $B$ . So, we take it to have a fixed value for now and then average over it later when we trace out the auxiliary modes. For simplicity, the state of the auxiliary modes isn't explicitly displayed here.

The most general pure input state of field  $A$  is given by

$$|\psi_{\text{in}}\rangle = \alpha |0\rangle + \beta |1\rangle \quad (3.3)$$

$$= \alpha |0\rangle + \beta \int dt \psi(t) |t\rangle \quad (3.4)$$

$$= \left( \alpha + \beta \int dt \psi(t) \hat{E}_A^{\text{in}\dagger}(t) \right) |0\rangle. \quad (3.5)$$

Now, employing our inverted input-output relation, we find

$$|\psi_{\text{out}}\rangle = \left( \alpha + \beta \int dt \psi(t) e^{i\hat{\xi}_A(t)} \hat{E}_A^{\text{out}\dagger}(t) \right) |0\rangle \quad (3.6)$$

$$= \alpha |0\rangle + \beta \int dt \psi(t) e^{i\hat{\xi}_A(t)} |t\rangle. \quad (3.7)$$

Taking the outer-product of this state with itself, and then tracing over the auxiliary modes (i.e. averaging over the phase noise), we obtain the actual output density operator:

$$\rho_{\text{out}} = \text{tr}_{\text{aux}}(|\psi_{\text{out}}\rangle\langle\psi_{\text{out}}|) \quad (3.8)$$

$$\begin{aligned} &= |\alpha|^2 |0\rangle\langle 0| + \alpha\beta^* \int dt \langle e^{i\hat{\xi}_A(t)} \rangle^* \psi^*(t) |0\rangle\langle t| + \alpha^*\beta \int dt \langle e^{i\hat{\xi}_A(t)} \rangle \psi(t) |t\rangle\langle 0| \\ &\quad + \int dt \int ds |\psi(t)|^2 |\psi(s)|^2 \langle e^{i(\hat{\xi}_A(t) - \hat{\xi}_A(s))} \rangle |t\rangle\langle s|. \end{aligned} \quad (3.9)$$

Taking the overlap with the input state, we have

$$\begin{aligned} \langle \psi_{\text{in}} | \rho_{\text{out}} | \psi_{\text{in}} \rangle &= |\alpha|^4 + 2|\alpha|^2|\beta|^2 \Re \left( \int dt \langle e^{i\hat{\xi}_A(t)} \rangle |\psi(t)|^2 \right) \\ &\quad + |\beta|^4 \int dt \int ds |\psi(t)|^2 |\psi(s)|^2 \langle e^{i(\hat{\xi}_A(t) - \hat{\xi}_A(s))} \rangle. \end{aligned} \quad (3.10)$$

Finally, the vacuum fidelity is obtained by averaging the input state—i.e.  $\alpha$  and  $\beta$ —over the uniform distribution on the Bloch sphere:

$$F_0 = \langle \langle \psi_{\text{in}} | \rho_{\text{out}} | \psi_{\text{in}} \rangle \rangle_{\alpha, \beta} \quad (3.11)$$

$$= \frac{1}{3} \left[ 1 + \Re \left( \int dt \langle e^{i\hat{\xi}_A(t)} \rangle |\psi(t)|^2 \right) + \int dt \int ds |\psi(t)|^2 |\psi(s)|^2 \langle e^{i(\hat{\xi}_A(t) - \hat{\xi}_A(s))} \rangle \right]. \quad (3.12)$$

## 3.2 Response-Independent Results

The two averages in Equation (3.12) can be calculated using our theory of continuous-time XPM. In particular, since the autocorrelation function for XPM with differing group velocities is identical to that for XPM with equal group velocities, Equation (1.7), these averages are the same as those given by Shapiro [12]:

$$\langle e^{i\hat{\xi}_A(t)} \rangle = e^{-\int \frac{d\omega}{4\pi} S_{\xi\xi}(\omega)} \quad (3.13)$$

$$\langle e^{i(\hat{\xi}_A(t) - \hat{\xi}_A(s))} \rangle = e^{-\int \frac{d\omega}{\pi} S_{\xi\xi}(\omega) \sin^2[\omega(t-s)/2]}. \quad (3.14)$$

One can plug these in, and then, given a response function, evaluate the vacuum fidelity and obtain a numeric result. However, before doing so, let's make a few strictly optimistic assumptions to obtain a simple upper bound. First, let's let the third term in Equation (3.12) go to 1, which is easily seen to be its maximum possible value and achieved in the absence of phase noise. Next, noting that  $\langle e^{i\hat{\xi}_A(t)} \rangle$  is upper bounded at  $T = 0$  K, let's assume that we are working at absolute zero. What we

are left with then is a simpler, maximum vacuum fidelity:

$$F_0^{\max} = \frac{2}{3} + \frac{1}{3}e^{-\frac{\eta L}{4\pi}\|H_{\text{im}}\|_1}, \quad (3.15)$$

where  $\|H_{\text{im}}\|_1 = \int_{-\infty}^{\infty} d\omega |H_{\text{im}}(\omega)|$  is the L1 norm of the imaginary part of the frequency response. Plugging in our uniform-phase-shift conditions, specifically Equation (2.19), we have

$$F_0^{\max} = \frac{2}{3} + \frac{1}{3}e^{-\frac{\phi}{2\pi}(t_h+t_\psi)\|H_{\text{im}}\|_1}. \quad (3.16)$$

(Note, restricting the inequalities in our uniform phase conditions, Equation (2.16), to equalities, Equations (2.17) and (2.19), only improves the vacuum fidelity.)

From the preceding result, we can draw a number of conclusions. First, it is readily apparent that the vacuum fidelity decreases as the phase shift increases. Moreover, it is clear that perfect fidelity is impossible, *even in theory*, for any physically valid response function, because such response functions are causal and non-instantaneous: For perfect fidelity, the argument of the exponent must be 0, which necessitates that either of  $(t_h + t_\psi)$  or  $\|H_{\text{im}}\|_1$  be 0. The former can't be 0 for non-instantaneous pulse shapes and response functions. The latter cannot be 0 for causal response functions, as  $\|H_{\text{im}}\|_1 = 0$  would imply an even response function in the time domain. The only exception then, is if we are willing to let  $\phi$  go to 0, which of course, misses the entire point we are working towards. Also, note that for a fixed material response, it is strictly optimistic to assume that we are working in the slow-response regime, i.e.  $t_\psi \ll t_h$ . Making this assumption, and assuming a  $\pi$ -radian phase shift, we are left with

$$F_0^{\max} = \frac{2}{3} + \frac{1}{3}e^{-\frac{1}{2}t_h\|H_{\text{im}}\|_1}. \quad (3.17)$$

### 3.3 Response-Dependent Results

One would think that we could put some analytic bounds on  $t_h \|H_{\text{im}}\|_1$ , independent of our choice of response function. This seems likely, but we have not been able to prove any such bound. So, from here, we are left with no choice but to examine a specific response function. In particular, let's study the single-resonance, two-pole response function studied by Shapiro [12], whose associated frequency response is

$$H(\omega) = \frac{\omega_0^2}{\omega_0^2 - \omega^2 - i\omega\gamma}. \quad (3.18)$$

For  $0 < \gamma/2 < \omega_0$ , the response function  $h(t)$  is underdamped:

$$h(t) = \frac{\omega_0^2 e^{-\frac{\gamma}{2}t} \sin\left(\sqrt{\omega_0^2 - \frac{\gamma^2}{4}}t\right)}{\sqrt{\omega_0^2 - \frac{\gamma^2}{4}}}, \text{ for } t \geq 0, \quad (3.19)$$

for  $\gamma/2 = \omega_0$  it is critically damped:

$$h(t) = \omega_0^2 t e^{-\omega_0 t}, \text{ for } t \geq 0, \quad (3.20)$$

and for  $\gamma/2 > \omega_0$  it is overdamped:

$$h(t) = \frac{\omega_0^2 e^{-\frac{\gamma}{2}t} \sinh\left(\sqrt{\frac{\gamma^2}{4} - \omega_0^2}t\right)}{\sqrt{\frac{\gamma^2}{4} - \omega_0^2}}, \text{ for } t \geq 0. \quad (3.21)$$

This response function actually has infinite duration; however, it will suffice to take  $t_h$  to be some reasonable measure of most of its duration. Noting that the fidelity decreases as  $t_h$  increases (all other things held constant), we optimistically take  $t_h$  to be the root-mean-square (RMS) average of  $h(t)$ :

$$t_h = \sqrt{\frac{\int_0^\infty dt t^2 h^2(t)}{\int_0^\infty dt h^2(t)} - \left(\frac{\int_0^\infty dt t h^2(t)}{\int_0^\infty dt h^2(t)}\right)^2} \quad (3.22)$$

$$= \sqrt{\frac{1}{\gamma^2} + \frac{\gamma^2}{4\omega_0^4} - \frac{1}{2\omega_0^2}}, \quad (3.23)$$

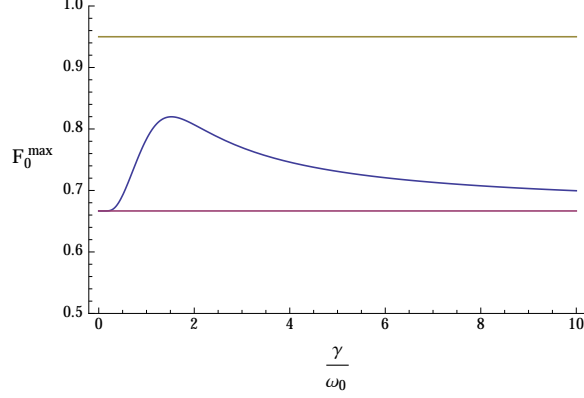


Figure 3-1: A plot of the maximum vacuum fidelity vs. the damping parameter of the single-resonance, two-pole response. The pink line denotes  $2/3$ , and the yellow line denotes  $0.95$ .

or, introducing the dimensionless parameter  $\Gamma = \gamma/\omega_0$ ,

$$\omega_0 t_h = \sqrt{\frac{1}{\Gamma^2} + \frac{\Gamma^2}{4} - \frac{1}{2}}. \quad (3.24)$$

This RMS duration,  $t_h$ , is minimized at  $\Gamma = \sqrt{2}$ , a little bit into the underdamped regime. Introducing another dimensionless parameter,  $\Omega = \omega/\omega_0$ , we have

$$\frac{||H_{\text{im}}||}{\omega_0} = \int_{-\infty}^{\infty} d\Omega \left| \frac{\Gamma \Omega}{\Gamma^2 \Omega^2 + (1 - \Omega^2)^2} \right| \quad (3.25)$$

$$= 2 \int_0^{\infty} d\Omega \frac{\Gamma \Omega}{\Gamma^2 \Omega^2 + (1 - \Omega^2)^2} \quad (3.26)$$

$$= -\frac{2 \tanh^{-1} \left( \frac{\Gamma^2 + 2\Omega^2 - 2}{\Gamma \sqrt{\Gamma^2 - 4}} \right)}{\sqrt{\Gamma^2 - 4}} \Bigg|_{\Omega=0}^{\Omega=\infty} \quad (3.27)$$

$$= \frac{\pi i + 2 \tanh^{-1} \left( \frac{\Gamma^2 - 2}{\Gamma \sqrt{\Gamma^2 - 4}} \right)}{\sqrt{\Gamma^2 - 4}}. \quad (3.28)$$

With these results in place, we can now evaluate Equation (4.22). A plot of  $F_0^{\text{max}}$  vs.  $\Gamma$  is shown in Figure 3-1. From this plot, it is clear that the vacuum fidelity cannot be very high. Numerically maximizing, we find the peak to be just less than 82%. It is worth emphasizing again that this itself is a very generous upper bound: it does not include noise due to self-phase modulation or other sources; it assumes operation at absolute zero; it assumes operation in the slow-response regime (which is most



certainly not true of fiber unless sub-femtosecond pulse durations are employed); we have been generous in our characterization of  $t_h$  by taking it to be the RMS deviation of the response; and we have generously set the third term of Equation (3.12) to 1, thus ignoring any fidelity degrading contributions it too will make. Accordingly, it seems fair to say then that, at least for this response function, that XPM is not useful for constructing a  $\pi$ -radian CPHASE gate.

A critical reader might dismiss this result as of little importance, due to its reliance on such a specific family of response functions. However, it is worth noting that historically an underdamped, single-resonance, two-pole response function has been used as a coarse approximation to the response of fused-silica fiber when analyzing Raman-scattering-induced noise [9, 11], and experimental measurements of the actual response for fused-silica fiber indeed demonstrate that such an approximation is not unreasonable [17]. So, despite the fact that the results of this section are response-dependent, they still carry immediate, practical consequences, and make a very strong case that the cross-Kerr effect alone is not useful in constructing a CPHASE gate.

To add to that strength, we note that Shapiro [12] also examined a related fidelity for the  $A$  field's output state, viz., one where field  $B$  is taken to contain a single photon and the overlap of the output state of field  $A$  is taken with its ideally-phase-shifted input state. This can be derived in a manner very similar to the derivation of the vacuum fidelity presented earlier, and is given by

$$F_1 = \frac{1}{3} \left[ 1 + \Re \left( e^{-i\phi} \int dt \langle e^{i\hat{\xi}_A(t)} \rangle \langle e^{i\hat{\zeta}_A(t)} \rangle |\psi(t)|^2 \right) + \int dt \int ds |\psi(t)|^2 |\psi(s)|^2 \langle e^{i(\hat{\xi}_A(t) - \hat{\xi}_A(s))} \rangle \right]. \quad (3.29)$$

So, for a uniform  $\phi$ -radian phase shift, it is clear that  $F_1 = F_0$ , and we get

$$F_1^{\max} = \frac{2}{3} + \frac{1}{3} e^{-\frac{\phi}{2\pi}(t_h + t_\psi) \|H_{\text{im}}\|_1}, \quad (3.30)$$

implying the same results we found for the vacuum fidelity.



# Chapter 4

## Principal-Mode Projection

While evidence presented thus far suggests that a high-fidelity bulk  $\pi$ -radian conditional phase shift is not attainable with XPM at the single-photon level, an intriguing possibility remains, which is to attempt to incrementally build up such a conditional phase shift with some form of error correction. In particular, a technique for doing this was developed by Chudzicki et al. [18] and dubbed “principal-mode projection”. Principal-mode projection (PMP) leverages a quantum Zeno effect to build up a large, high-fidelity phase shift by cascading a number of smaller phase shifts and projecting out the error in between each cascade. If the trade-off between error and phase-shift strength is favorable, then a high-fidelity  $\pi$ -radian phase shift can be achieved. Chudzicki et al. applied this concept to a system in which photons interact with a V-type atomic system in a one-sided cavity, and found that the error scaling for the system was favorable enough to support PMP: increasingly high fidelity could be obtained with a polynomial number of cascades. So, we now apply this technique to XPM to see if it can enable a high-fidelity CPHASE.

### 4.1 Phase-Noise Injection as a Beam Splitter

To apply PMP to continuous-time XPM, it is useful to reframe XPM itself. So far, we have concerned ourselves with an input-output relation for the field operators at every instance in time. Instead, what we now must concern ourselves with is the evolution

of the *principal* mode, namely  $\psi(t)$ , the shape of our single-photon pulses. For now, we will only concern ourselves with calculating the vacuum fidelity. So, taking field  $B$  to be in the vacuum state, we would like to develop a Schrödinger evolution of the state of field  $A$ . Choosing any orthonormal basis of modes  $\{\psi_n(t)\}$ , we have that

$$\hat{E}_A(t) = \sum_n \psi_n(t) \hat{a}_n \quad (4.1)$$

Taking the first mode to be our principal mode,  $\psi(t)$ , and the remaining modes to be some set of modes  $\{\phi_n(t)\}$  that together with  $\psi(t)$  forms an orthonormal basis, we have

$$\hat{E}_A(t) = \psi(t) \hat{a}_\psi + \sum_n \phi_n(t) \hat{a}_n. \quad (4.2)$$

Now, what we care about is an input-output relation for  $\hat{a}_\psi$ , which we can then use to find the Schrödinger evolution of the input state. Noting that field  $B$  is in vacuum, we have

$$\hat{E}_A^{\text{out}}(t) = e^{i\hat{\xi}_A(t)} \hat{E}_A^{\text{in}}(t). \quad (4.3)$$

Following the same procedure as the derivation of the vacuum fidelity in Chapter 3, we can treat  $\hat{\xi}_A(t)$  as a classical random process since the auxiliary modes it operates on are entirely independent from the optical fields. We'll assume that  $\xi_A(t)$ , the classical version of  $\hat{\xi}_A(t)$ , is known for now, and then average our output state over

it at the end. With this in mind we have

$$\hat{E}_A^{\text{out}}(t) = e^{i\xi_A(t)} \hat{E}_A^{\text{in}}(t) \quad (4.4)$$

$$\int dt \psi^*(t) \hat{E}_A^{\text{out}}(t) = \int dt \psi^*(t) e^{i\xi_A(t)} \hat{E}_A^{\text{in}}(t) \quad (4.5)$$

$$\hat{a}_\psi^{\text{out}} = \hat{a}_\psi^{\text{in}} \int dt |\psi(t)|^2 e^{i\xi_A(t)} + \sum_n \hat{a}_n^{\text{in}} \int dt \psi^*(t) \phi_n(t) e^{i\xi_A(t)} \quad (4.6)$$

$$\begin{aligned} \hat{a}_\psi^{\text{out}} &= \hat{a}_\psi^{\text{in}} \int dt |\psi(t)|^2 e^{i\xi_A(t)} \\ &\quad + \hat{a}_{\text{sc}}^{\text{in}} \sqrt{1 - \int ds \int dt |\psi(t)|^2 |\psi(s)|^2 e^{i(\xi_A(s) - \xi_A(t))}}, \end{aligned} \quad (4.7)$$

where  $\hat{a}_{\text{sc}}$  is the appropriate linear combination of the  $\{\hat{a}_n\}$  associated with the  $\{\phi_n(t)\}$  modes. Note that  $[\hat{a}_{\text{sc}}, \hat{a}_{\text{sc}}^\dagger] = 1$ . Moreover, since our input photon exists only in the  $\psi(t)$  mode, and for PMP we only care about the same mode at the output (and will trace over all other modes), we can regard  $\hat{a}_{\text{sc}}$  to be the annihilation operator for a single scattered mode. So, we proceed forwards with this simplification as a convenience, but note as we move along that the calculations would end up exactly the same if we were to burden ourselves with the full set of modes.

Defining coefficients  $T \equiv \int dt |\psi(t)|^2 e^{i\xi_A(t)}$  and  $R \equiv \sqrt{1 - |T|^2}$ , Equation (4.7) becomes

$$\hat{a}_\psi^{\text{out}} = T \hat{a}_\psi^{\text{in}} + R \hat{a}_{\text{sc}}^{\text{in}}, \quad (4.8)$$

which is precisely a beam splitter input-output relation, assuming the configuration of Figure 4-1. This makes good physical sense; the phase noise can be thought of as scattering our input photon out of the principal temporal mode. (The transmissivity of this hypothetical beam splitter is a classical random variable.) So, without thinking much more, it is clear that

$$\hat{a}_\psi^{\text{in}\dagger} = T \hat{a}_\psi^{\text{out}\dagger} - R^* \hat{a}_{\text{sc}}^{\text{out}\dagger}. \quad (4.9)$$

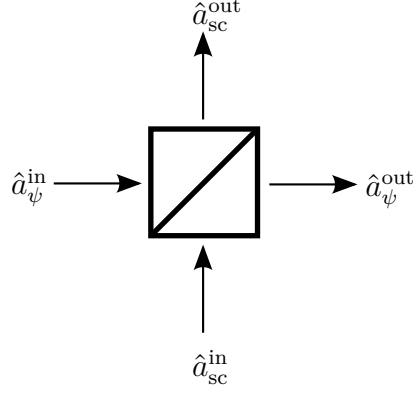


Figure 4-1: A beam splitter whose input-output relation is analogous to the phase-noise injection of XPM.

The input state of field  $A$  is given by

$$|\psi_{\text{in}}\rangle = (\alpha |0\rangle_\psi + \beta |1\rangle_\psi) |0\rangle_{\text{sc}} \quad (4.10)$$

$$= (\alpha + \beta \hat{a}_\psi^{\text{in}\dagger}) |0\rangle_\psi |0\rangle_{\text{sc}}. \quad (4.11)$$

Using Equation (4.9), we find that the output state conditioned on knowledge of the phase noise is given by

$$|\psi_{\text{out}}\rangle = (\alpha + \beta(T\hat{a}_\psi^{\text{out}\dagger} - R^*\hat{a}_{\text{sc}}^{\text{out}\dagger})) |0\rangle_\psi |0\rangle_{\text{sc}} \quad (4.12)$$

$$= \alpha |0\rangle_\psi |0\rangle_{\text{sc}} + \beta T |1\rangle_\psi |0\rangle_{\text{sc}} - \beta R^* |0\rangle_\psi |1\rangle_{\text{sc}}. \quad (4.13)$$

Taking the outer product of this state with itself and averaging over the phase noise would yield the unconditional output-state density operator of the XPM interaction, bearing in mind that we have oversimplified our treatment of the scattered modes. To find the output of the XPM+PMP interaction then, we merely have to follow the aforementioned calculation with tracing out the scattered mode. (It is this tracing out that justifies our lumping the linear combination of all the  $\{\phi_n(t)\}$  modes into a single temporal mode with annihilation operator  $\hat{a}_{\text{sc}}$ .) Carrying out this calculation,

we have

$$\rho_{\psi}^{\text{out}} = \text{tr}_{\text{sc}}(\langle |\psi_{\text{out}}\rangle \langle \psi_{\text{out}}| \rangle) \quad (4.14)$$

$$\begin{aligned} &= (|\alpha|^2 + |\beta|^2 \langle |R|^2 \rangle) |0\rangle_{\psi} \langle 0|_{\psi} + \alpha\beta^* \langle T^* \rangle |0\rangle_{\psi} \langle 1|_{\psi} + \alpha^* \beta \langle T \rangle |1\rangle_{\psi} \langle 0|_{\psi} \\ &\quad + |\beta|^2 \langle |T|^2 \rangle |1\rangle_{\psi} \langle 1|_{\psi} \end{aligned} \quad (4.15)$$

$$\begin{aligned} &= (1 - |\beta|^2 \langle |T|^2 \rangle) |0\rangle_{\psi} \langle 0|_{\psi} + \alpha\beta^* \langle T^* \rangle |0\rangle_{\psi} \langle 1|_{\psi} + \alpha^* \beta \langle T \rangle |1\rangle_{\psi} \langle 0|_{\psi} \\ &\quad + |\beta|^2 \langle |T|^2 \rangle |1\rangle_{\psi} \langle 1|_{\psi}. \end{aligned} \quad (4.16)$$

The result of this process is an XPM operation that can be cascaded; the principal mode is left in the mixed-state given by Equation (4.16) and it is assumed that the scattered modes will be left in the vacuum state, just as they were at the input. How exactly PMP is carried out in practice, i.e. how exactly the fraction of a photon in the scattered modes is thrown away, is not important, although the procedure presented by Chudzicki et al. [18] serves as a possibility.

## 4.2 The Effect of PMP on Fidelity without Cascading

Our objective, in the rest of this chapter, is to evaluate the vacuum fidelity that results from  $N$  cascades of the XPM+PMP operation from the previous section. We begin, here, by obtaining the vacuum fidelity for a single iteration of XPM+PMP. It is found as follows:

$$F_0 = \langle (\alpha^* \langle 0| + \beta^* \langle 1|) \rho_{\psi}^{\text{out}} (\alpha |0\rangle + \beta |1\rangle) \rangle_{\alpha, \beta} \quad (4.17)$$

$$= \langle |\alpha|^2 - |\alpha|^2 |\beta|^2 \langle |T|^2 \rangle + 2|\alpha|^2 |\beta|^2 \langle \Re(T) \rangle + |\beta|^4 \langle |T|^2 \rangle \rangle_{\alpha, \beta} \quad (4.18)$$

$$= \frac{1}{2} + \frac{1}{3} \langle \Re(T) \rangle + \frac{1}{6} \langle |T|^2 \rangle \quad (4.19)$$

$$= \frac{1}{2} + \frac{1}{3} \langle \Re \left( \int dt |\psi(t)|^2 e^{i\xi_A(t)} \right) \rangle + \frac{1}{6} \left\langle \int ds \int dt |\psi(t)|^2 |\psi(s)|^2 e^{i\xi_A(s) - i\xi_A(t)} \right\rangle \quad (4.20)$$

$$= \frac{1}{2} + \frac{1}{3} \langle e^{i\xi_A(t)} \rangle + \frac{1}{6} \int ds \int dt |\psi(t)|^2 |\psi(s)|^2 \langle e^{i(\xi_A(s) - \xi_A(t))} \rangle, \quad (4.21)$$

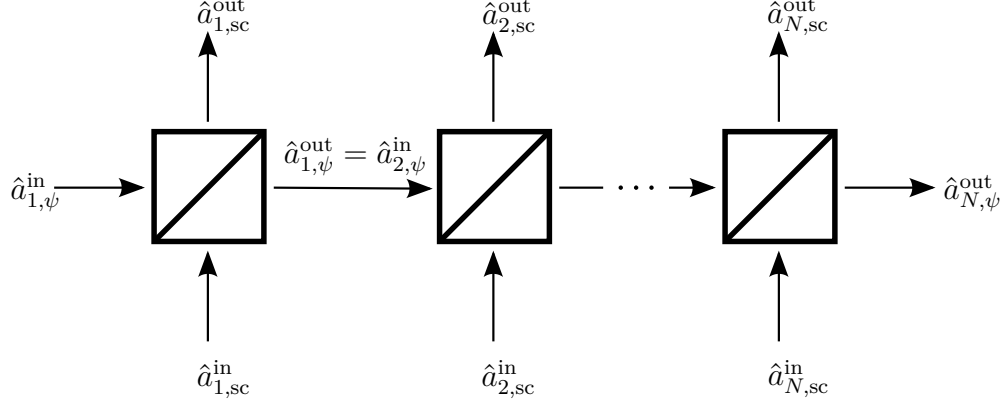


Figure 4-2: A train of beam splitters, analogous to the phase-noise behavior of cascading  $N$  XPM+PMP elements.

where, as before,  $\langle \cdot \rangle_{\alpha, \beta}$  denotes averaging  $\alpha$  and  $\beta$  over the uniform distribution on the Bloch sphere, and we have used the fact that  $\langle e^{i\xi_A(t)} \rangle$  is real. Comparing against Equation (3.12), the vacuum fidelity for XPM without PMP, we see that PMP *does* help. Interpreting the phase noise as a scattering, there are two sources of error in the vacuum fidelity: not enough photon in the principal mode, and too much photon in the scattered modes. PMP helps by eliminating the second source of error. However, it is evident that it doesn't help enough, because by being optimistic and setting the third term equal to 1, we are left with the same maximum vacuum fidelity, regardless of whether or not we employ PMP:

$$F_0^{\max} = \frac{2}{3} + \frac{1}{3} \langle T \rangle = \frac{2}{3} + \frac{1}{3} \langle e^{i\xi_A(t)} \rangle. \quad (4.22)$$

We have already seen that this fidelity cannot be made high. So, it follows that PMP cannot save the situation, at least not with one iteration.

### 4.3 Cascading PMP

What remains, in order to determine whether PMP might enable a high-fidelity CPHASE gate, is to analyze the situation in which we cascade  $N$  XPM+PMP op-



erations, each with the strength to impart a fractional phase shift  $\phi_i$  (were field  $B$  to contain a photon), where these fractional phase shifts sum up to the total desired phase shift  $\phi = \sum_i \phi_i$ , which ultimately we will take to be  $\pi$ . Interpreting the phase noise as a beam splitter and PMP as throwing out (tracing over) the scattered mode(s), this scenario is depicted in Figure 4-2. Each scattered-mode input is in the vacuum state, each scattered-mode output is discarded, the computational input state is fed into the principal mode at the left, and the final computational output state is taken from the principal mode at the right. Each beam splitter has a transmissivity  $T_i$  that is a classical random variable summarizing the scattering induced by the phase noise from that chunk of XPM material, and these random variables are statistically independent since the XPM materials are independent. From Figure 4-2 it is immediately clear that this train of beam splitters, ignoring the scattered outputs, is no different than a single beam splitter with transmissivity  $T = \prod_{i=1}^N T_i$ :

$$\hat{a}_{N,\psi}^{\text{out}} = \left( \prod_{i=1}^N T_i \right) \hat{a}_{1,\psi}^{\text{in}} + \dots \quad (4.23)$$

From this, it is clear that a cascade of  $N$  XPM+PMP operations will still have a vacuum fidelity limited by the maximum vacuum fidelity in Equation (4.22), where  $\langle T \rangle$  is now given by  $\langle T \rangle = \langle \prod_{i=1}^N T_i \rangle = \prod_{i=1}^N \langle T_i \rangle$ . But note,

$$\prod_{i=1}^N \langle T_i \rangle = \prod_{i=1}^N \langle e^{i\xi_{i,A}(t)} \rangle \quad (4.24)$$

$$= \prod_{i=1}^N e^{\frac{\phi_i}{2\pi}(t_h+t_\psi)\|H_{\text{im}}\|_1} \quad (4.25)$$

$$= e^{\frac{1}{2\pi}(\sum_{i=1}^N \phi_i)(t_h+t_\psi)\|H_{\text{im}}\|_1} \quad (4.26)$$

$$= e^{\frac{\phi}{2\pi}(t_h+t_\psi)\|H_{\text{im}}\|_1} \quad (4.27)$$

$$= \langle e^{i\xi_A(t)} \rangle. \quad (4.28)$$

That is to say, the error and phase shift scale in essentially the same way, the number of cascades has no effect on the maximum vacuum fidelity.

Also, note that by taking  $T \equiv \int dt |\psi(t)|^2 e^{i\hat{\xi}_A(t)} e^{i\hat{\xi}_A(t)}$  and making one sign change,

we can adopt our vacuum-fidelity calculation to obtain the  $F_1$  fidelity for XPM+PMP (and, by essentially the same analysis as above, an arbitrary number of cascades):

$$F_1 = \frac{1}{2} + \frac{1}{3} \langle e^{-i\phi} \Re(T) \rangle + \frac{1}{6} \langle |T|^2 \rangle \quad (4.29)$$

$$\begin{aligned} &= \frac{1}{2} + \frac{1}{3} \langle e^{i\hat{\xi}_A(t)} \rangle \Re(e^{-i\phi} \int dt |\psi(t)|^2 \langle e^{i\hat{\zeta}_A(t)} \rangle) \\ &\quad + \frac{1}{6} \int ds \int dt |\psi(t)|^2 |\psi(s)|^2 \langle e^{i(\hat{\zeta}_A(s) - \hat{\zeta}_A(t))} \rangle \langle e^{i(\xi_A(s) - \xi_A(t))} \rangle. \end{aligned} \quad (4.30)$$

Unsurprisingly, we see that, as in the no-PMP case, this is equivalent to the vacuum fidelity if we assume a uniform phase shift.

What we can take away from all this is that PMP, while it does help, does not fundamentally alter the fidelity-degrading phase noise, and has essentially no effect on our analysis of XPM. That is to say, even PMP with an *arbitrary* number of cascades, cannot save XPM as the route to a high-fidelity all-optical CPHASE gate.

# Chapter 5

## Conclusions and Future Work

Taken as a whole, this work casts a dark shadow on the prospect of leveraging the cross-Kerr effect to perform universal quantum computation. The results presented in this thesis show that even under a large set of favorable assumptions—absolute-zero temperature, operation in the slow-response regime, making use of incremental error-correction, etc.—the fidelity of a  $\pi$ -radian conditional phase shift cannot be made high, even when single-photon pulses propagate through each other. This result does, however, depend on analysis carried out on a specific family of response functions. So, an avenue for future work would be to analyze the actual response for fused-silica fiber, or other materials, and possibly even make these results completely response-independent.

On a more hopeful note, recent results [18, 19], suggest that a high-fidelity  $\pi$ -radian conditional phase shift can be attained using cavity systems. Heuristically, one might imagine that surrounding an XPM material with a cavity could constrain the system so as not to allow for the multimode scattering (phase noise) that this thesis analyzes. So, developing a continuous-time theory of XPM for cavity-type systems constitutes a promising direction for future work.

Finally, a larger topic for future work would be to explore the extent to which these results apply to other systems, beyond nonlinear optics. It stands to reason that the phase noise analyzed in this thesis could prove to be a problem for any system in which the desired interaction happens in a multimode sense. Ultimately, what this

work has done, and future work built upon it should hope to do, is better constrain the problem space of universal quantum computing. As it stands, the number of possible avenues for building a universal quantum computer is so many so as to drain much time and money exploring them all. If we can see ahead which of these roads will ultimately lead to dead ends, and avoid them, perhaps we can make it to our destination sooner.

# Appendix A

## XPM with Counter-Propagating Pulses

### A.1 Classical XPM

To begin, we develop the classical theory of XPM for counter-propagating fields, i.e. fields with group velocities that are equal in magnitude but opposite in direction. Take  $E_A(z, t)$  and  $E_B(z, t)$  to be the fields of interest. Take  $E_A$  to be propagating in the  $+z$  direction with group velocity  $v$ , and similarly, take  $E_B$  to be propagating in the  $-z$  direction with the same group velocity. Finally, we take the region from  $z = 0$  to  $z = L$  to contain the XPM medium, understanding  $z = 0$  to be the input plane for mode  $A$  and the output plane for mode  $B$  and vice versa for  $z = L$ . In this scenario,  $E_A$  obeys the following differential equation in the interaction medium:

$$\left( \frac{\partial}{\partial z} + \frac{1}{v} \frac{\partial}{\partial t} \right) E_A(z, t) = i n_A(z, t) E_A(z, t). \quad (\text{A.1})$$

Here,  $n_A(z, t)$  is the intensity-dependent index of refraction of the interaction medium and is given by

$$n_A(z, t) = \eta \int_{-\infty}^{\infty} dt' h(t - t') I_B(z, t'), \quad (\text{A.2})$$

where  $I_B(z, t) = |E_B(z, t)|^2$  is the field intensity of the  $B$  field,  $h(t)$  is the causal, real-valued, normalized ( $\int_{-\infty}^{\infty} dt h(t) = 1$ ) XPM response function, and  $\eta$  characterizes the strength of the interaction.

From Equation (A.1), it is clear that the intensity of field  $A$  propagates as usual:

$$I_A(z, t) = I_A(0, t - z/v). \quad (\text{A.3})$$

By symmetry, for mode  $B$  we must have

$$I_B(z, t) = I_B(L, t - (L - z)/v). \quad (\text{A.4})$$

That is to say, the XPM interaction only affects the phase of the fields. This motivates the following change of variables to assist in solving for  $E_A$ :

$$\bar{z} = z, \quad \bar{t} = t - z/v. \quad (\text{A.5})$$

In terms of these coordinates, we have

$$\frac{\partial}{\partial z} + \frac{1}{v} \frac{\partial}{\partial t} = \left( \frac{\partial \bar{z}}{\partial z} \frac{\partial}{\partial \bar{z}} + \frac{\partial \bar{t}}{\partial z} \frac{\partial}{\partial \bar{t}} \right) + \frac{1}{v} \left( \frac{\partial \bar{z}}{\partial t} \frac{\partial}{\partial \bar{z}} + \frac{\partial \bar{t}}{\partial t} \frac{\partial}{\partial \bar{t}} \right) = \frac{\partial}{\partial \bar{z}}, \quad (\text{A.6})$$

which allows us to rewrite Equation (A.1) as

$$\frac{\partial}{\partial \bar{z}} \bar{E}_A(\bar{z}, \bar{t}) = i \bar{n}_A(\bar{z}, \bar{t}) \bar{E}_A(\bar{z}, \bar{t}). \quad (\text{A.7})$$

Here  $\bar{E}_A(\cdot, \cdot)$  denotes the functional form of the field in the new coordinates, defined as

$$\bar{E}_A(\bar{z}, \bar{t}) = E_A\left(z(\bar{z}, \bar{t}), t(\bar{z}, \bar{t})\right), \quad (\text{A.8})$$

and  $\bar{n}_A(\bar{z}, \bar{t})$  is defined analogously.

In this new form, we can easily solve for field  $A$ :

$$\overline{E}_A(\overline{z}, \overline{t}) = \overline{E}_A(0, \overline{t}) e^{i \int_0^{\overline{z}} d\overline{z}' \overline{n}_A(\overline{z}', \overline{t})}. \quad (\text{A.9})$$

Alternatively, in terms of the original coordinates,

$$E_A(L, t + L/v) = E_A(0, t) e^{i\zeta_A(t)}, \quad (\text{A.10})$$

where,

$$\begin{aligned} \zeta_A(t) &= \int_0^L dz \, n_A(z, t + z/v) \\ &= \eta \int_0^L dz \int_{-\infty}^{\infty} dt' \, h(t + z/v - t') I_B(z, t'). \end{aligned} \quad (\text{A.11})$$

Taking  $t'' = t' - z/v$  and making use of Equation (A.4), we can rewrite this as

$$\zeta_A(t) = \eta \int_0^L dz \int_{-\infty}^{\infty} dt'' \, h(t - t'') I_B(L, t'' + (2z - L)/v). \quad (\text{A.12})$$

By symmetry, flipping the roles of input and output, and reversing the direction of propagation, (i.e. substituting  $L - z$  for  $z$ ) the solution for mode  $B$  must be

$$E_B(0, t + L/v) = E_A(L, t) e^{i\zeta_B(t)}, \quad (\text{A.13})$$

with

$$\zeta_B(t) = \eta \int_0^L dz \int_{-\infty}^{\infty} dt'' \, h(t - t'') I_A(0, t'' - (2z - L)/v). \quad (\text{A.14})$$

Taking  $E_A^{\text{in}}(t) = E_A(0, t)$  and  $E_B^{\text{in}}(t) = E_B(L, t)$  to be the input fields and  $E_A^{\text{out}}(t) = E_A(L, t + L/v)$  and  $E_B^{\text{out}}(t) = E_B(0, t + L/v)$  to be the output fields, we can summarize

these results by the input-output relations:

$$E_A^{\text{out}}(t) = e^{i\zeta_A(t)} E_A^{\text{in}}(t), \quad (\text{A.15a})$$

$$E_B^{\text{out}}(t) = e^{i\zeta_B(t)} E_B^{\text{in}}(t). \quad (\text{A.15b})$$

## A.2 Quantum XPM

Turning to the quantum case, one would be tempted to toss carets on all instances (explicit and implicit) of  $E$  in Equation (A.15) and call it a day. However, as it turns out, this will not preserve the free-field commutator relations. Instead, as in the co-propagating theories, the correct input-output summary requires the introduction of phase-noise operators to preserve the commutators:

$$\hat{E}_A^{\text{out}}(t) = e^{i\hat{\xi}_A(t)} e^{i\hat{\zeta}_A(t)} \hat{E}_A^{\text{in}}(t), \quad (\text{A.16a})$$

$$\hat{E}_B^{\text{out}}(t) = e^{i\hat{\xi}_B(t)} e^{i\hat{\zeta}_B(t)} \hat{E}_B^{\text{in}}(t), \quad (\text{A.16b})$$

with appropriate definitions for the phase-noise operators  $\hat{\xi}_A(t)$  and  $\hat{\xi}_B(t)$  and with the phase-shift operators  $\hat{\zeta}_A(t)$  and  $\hat{\zeta}_B(t)$  given by putting carets on the fields in the definitions of their classical counterparts.

For the counter-propagating case, the phase-shift operators are given by

$$\hat{\zeta}_A(t) = \eta \int_0^L dz' \int_{-\infty}^{\infty} dt' h(t-t') \hat{I}_B^{\text{in}}(t' + (2z-L)/v) \quad (\text{A.17a})$$

$$\hat{\zeta}_B(t) = \eta \int_0^L dz' \int_{-\infty}^{\infty} dt' h(t-t') \hat{I}_A^{\text{in}}(t' - (2z-L)/v). \quad (\text{A.17b})$$

Taking a cue from Equation (1.5), we suggest the following definition of the phase-noise operators:

$$\hat{\xi}_A(t) = \int_0^L dz \int_0^{\infty} \frac{d\omega}{2\pi} \sqrt{\eta H_{\text{im}}(\omega)} \{ [\hat{B}(z, \omega) - i\hat{C}^\dagger(z, \omega)] e^{-i\omega(t+z/v)} + \text{hc} \}, \quad (\text{A.18a})$$

$$\hat{\xi}_B(t) = \int_0^L dz \int_0^{\infty} \frac{d\omega}{2\pi} \sqrt{\eta H_{\text{im}}(\omega)} \{ [\hat{B}(z, \omega) + i\hat{C}^\dagger(z, \omega)] e^{-i\omega(t+(L-z)/v)} + \text{hc} \}, \quad (\text{A.18b})$$



which will later be shown to be sufficient for preserving the necessary commutator relations. Here,  $\hat{B}(z, \omega)$  and  $\hat{C}(z, \omega)$  are a collection of space-frequency annihilation operators for auxiliary modes.  $\hat{B}$  and  $\hat{C}$  commute with each other over all frequencies and positions, and they obey the standard field commutator relations otherwise:

$$[\hat{B}(z, \omega), \hat{C}(z', \omega')] = [\hat{B}^\dagger(z, \omega), \hat{C}(z', \omega')] = 0 \quad (\text{A.19a})$$

$$[\hat{B}(z, \omega), \hat{B}(z', \omega')] = [\hat{C}(z, \omega), \hat{C}(z', \omega')] = 0 \quad (\text{A.19b})$$

$$[\hat{B}(z, \omega), \hat{B}^\dagger(z', \omega')] = [\hat{C}(z, \omega), \hat{C}^\dagger(z', \omega')] = 2\pi\delta(\omega - \omega')\delta(z - z'). \quad (\text{A.19c})$$

From this, it follows that

$$\begin{aligned} [\hat{\xi}_A(t), \hat{\xi}_B(s)] &= \int_0^L dz \int_0^L dz' \int_0^\infty \frac{d\omega}{2\pi} \int_0^\infty \frac{d\omega'}{2\pi} \sqrt{\eta H_{\text{im}}(\omega)} \sqrt{\eta H_{\text{im}}(\omega')} \\ &\quad 2(e^{-i\omega(t+z/v)} e^{i\omega'(s+(L-z')/v)} - \text{hc}) 2\pi\delta(\omega - \omega')\delta(z - z') \\ &= 2i\eta \int_0^L dz \int_0^\infty \frac{d\omega}{\pi} H_{\text{im}}(\omega) \sin(\omega(s - t - (2z - L)/v)), \end{aligned}$$

where we have taken  $H_{\text{im}}(\omega) \geq 0$  for  $\omega \geq 0$ . Now, using standard properties of Fourier transforms of even parts of functions, we have

$$[\hat{\xi}_A(t), \hat{\xi}_B(s)] = i\eta \int_0^L dz [h(s - t - (2z - L)/v) - h(t - s + (2z - L)/v)]. \quad (\text{A.20})$$

Turning to the symmetrized autocorrelation function, we have

$$\begin{aligned} \langle \{\hat{\xi}_A(t), \hat{\xi}_A(s)\} \rangle &= \\ &\int_0^L dz \int_0^L dz' \int_0^\infty \frac{d\omega}{2\pi} \int_0^\infty \frac{d\omega'}{2\pi} \sqrt{\eta H_{\text{im}}(\omega)} \sqrt{\eta H_{\text{im}}(\omega')} \\ &\quad (e^{-i\omega(t+z/v) - i\omega'(s+z'/v)} \langle \{\hat{B}(z, \omega) - i\hat{C}^\dagger(z, \omega), \hat{B}(z', \omega') - i\hat{C}^\dagger(z', \omega')\} \rangle \\ &\quad + e^{-i\omega(t+z/v) + i\omega'(s+z'/v)} \langle \{\hat{B}(z, \omega) - i\hat{C}^\dagger(z, \omega), \hat{B}^\dagger(z', \omega') + i\hat{C}(z', \omega')\} \rangle \\ &\quad + e^{i\omega(t+z/v) - i\omega'(s+z'/v)} \langle \{\hat{B}^\dagger(z, \omega) + i\hat{C}(z, \omega), \hat{B}(z', \omega') - i\hat{C}^\dagger(z', \omega')\} \rangle \\ &\quad + e^{i\omega(t+z/v) + i\omega'(s+z'/v)} \langle \{\hat{B}^\dagger(z, \omega) + i\hat{C}(z, \omega), \hat{B}^\dagger(z', \omega') + i\hat{C}(z', \omega')\} \rangle). \end{aligned} \quad (\text{A.21})$$

Taking  $\hat{B}$  and  $\hat{C}$  to be in independent thermal states, many of these terms can be eliminated because

$$\langle \hat{B}(z, \omega) \hat{B}(z', \omega') \rangle = \langle \hat{C}(z, \omega) \hat{C}(z', \omega') \rangle = \langle \hat{B}(z, \omega) \hat{C}^\dagger(z', \omega') \rangle = 0, \quad (\text{A.22})$$

and the conjugates of such terms likewise go to zero. Simplifying Equation (A.21), we have

$$\begin{aligned} \langle \{ \hat{\xi}_A(t), \hat{\xi}_A(s) \} \rangle &= \int_0^L dz \int_0^L dz' \int_0^\infty \frac{d\omega}{2\pi} \int_0^\infty \frac{d\omega'}{2\pi} \sqrt{\eta H_{\text{im}}(\omega)} \sqrt{\eta H_{\text{im}}(\omega')} \\ &\quad e^{-i\omega(t+z/v) + i\omega'(s+z'/v)} \langle \{ \hat{B}(z, \omega), \hat{B}^\dagger(z', \omega') \} + \{ \hat{C}^\dagger(z, \omega), \hat{C}(z', \omega') \} \rangle \\ &\quad + e^{i\omega(t+z/v) - i\omega'(s+z'/v)} \langle \{ \hat{B}^\dagger(z, \omega), \hat{B}(z', \omega') \} + \{ \hat{C}(z, \omega), \hat{C}^\dagger(z', \omega') \} \rangle \\ &= \int_0^L dz \int_0^L dz' \int_0^\infty \frac{d\omega}{2\pi} \int_0^\infty \frac{d\omega'}{2\pi} \sqrt{\eta H_{\text{im}}(\omega)} \sqrt{\eta H_{\text{im}}(\omega')} \\ &\quad (e^{-i\omega(t+z/v) + i\omega'(s+z'/v)} + e^{i\omega(t+z/v) - i\omega'(s+z'/v)}) \\ &\quad \langle \{ \hat{B}(z, \omega), \hat{B}^\dagger(z', \omega') \} + \{ \hat{C}(z, \omega), \hat{C}^\dagger(z', \omega') \} \rangle. \end{aligned} \quad (\text{A.23})$$

From the field commutator relations, we have

$$\{ \hat{B}(z, \omega), \hat{B}^\dagger(z', \omega') \} = 2\pi\delta(z - z')\delta(\omega - \omega') + 2\langle \hat{B}^\dagger(z, \omega) \hat{B}(z', \omega') \rangle \quad (\text{A.24a})$$

$$\{ \hat{C}(z, \omega), \hat{C}^\dagger(z', \omega') \} = 2\pi\delta(z - z')\delta(\omega - \omega') + 2\langle \hat{C}^\dagger(z, \omega) \hat{C}(z', \omega') \rangle, \quad (\text{A.24b})$$

and from the thermal-state nature of the auxiliary modes we have

$$\langle \hat{B}^\dagger(z, \omega) \hat{B}(z', \omega') \rangle = \langle \hat{C}^\dagger(z, \omega) \hat{C}(z', \omega') \rangle = \frac{1}{e^{\frac{\hbar\omega}{k_B T}} - 1} 2\pi\delta(z - z')\delta(\omega - \omega'). \quad (\text{A.25})$$

Making use of these facts, we have

$$\begin{aligned} \langle \{\hat{\xi}_A(t), \hat{\xi}_A(s)\} \rangle &= \int_0^L dz \int_0^L dz' \int_0^\infty \frac{d\omega}{2\pi} \int_0^\infty \frac{d\omega'}{2\pi} \sqrt{\eta H_{\text{im}}(\omega)} \sqrt{\eta H_{\text{im}}(\omega')} \\ &\quad (e^{-i\omega(t+z/v)+i\omega'(s+z'/v)} + e^{i\omega(t+z/v)-i\omega'(s+z'/v)}) \\ &\quad 2(1 + \frac{2}{e^{\frac{\hbar\omega}{k_B T}} - 1}) 2\pi \delta(z - z') \delta(\omega - \omega') \end{aligned} \quad (\text{A.26})$$

$$= \eta \int_0^L dz \int_0^\infty \frac{d\omega}{\pi} H_{\text{im}}(\omega) 2 \cos(\omega(t - s)) \frac{1 + e^{\frac{\hbar\omega}{k_B T}}}{e^{\frac{\hbar\omega}{k_B T}} - 1} \quad (\text{A.27})$$

$$= 2\eta L \int_0^\infty \frac{d\omega}{\pi} H_{\text{im}}(\omega) \cos(\omega(t - s)) \coth \left[ \frac{\hbar\omega}{2k_B T} \right]. \quad (\text{A.28})$$

Making use of the fact that  $H_{\text{im}}(\omega)$  is odd and  $\kappa = \eta L$ , and noting that this derivation would carry through the same way for mode  $B$ , we have exactly the same result as the co-propagating case:  $\hat{\xi}_A(t)$  and  $\hat{\xi}_B(t)$  are in jointly-Gaussian states with symmetrized autocorrelation functions

$$\langle \{\hat{\xi}_A(t), \hat{\xi}_A(s)\} \rangle = \langle \{\hat{\xi}_B(t), \hat{\xi}_B(s)\} \rangle = \int_{-\infty}^\infty \frac{d\omega}{\pi} S_{\xi\xi}(\omega) \cos[\omega(t - s)] \quad (\text{A.29a})$$

$$S_{\xi\xi}(\omega) = \kappa H_{\text{im}}(\omega) \coth \left[ \frac{\hbar\omega}{2k_B T} \right]. \quad (\text{A.29b})$$

With the properties of the noise operators squared away, we can now turn our attention to the issue of commutator preservation. First note that we have  $[\hat{\xi}_K(t), \hat{\xi}_K(s)] = [\hat{\zeta}_K(t), \hat{\zeta}_K(s)] = 0$  for  $K \in \{A, B\}$  where the former follows from the commutator relations for  $\hat{B}$  and  $\hat{C}$ , and the latter follows from the fact that  $[\hat{I}_K^{\text{in}}(t), \hat{I}_K^{\text{in}}(s)] = 0$ . From these relations it is clear that  $[\hat{E}_K^{\text{out}}(t), \hat{E}_K^{\text{out}\dagger}(s)] = \delta(t - s)$ . Moreover, it is not hard to see that we also have  $[\hat{E}_K^{\text{out}}(t), \hat{E}_K^{\text{out}}(s)] = 0$ . What remains then is to show  $[\hat{E}_A^{\text{out}}(t), \hat{E}_B^{\text{out}}(s)] = [\hat{E}_A^{\text{out}}(t), \hat{E}_B^{\text{out}\dagger}(s)] = 0$ . We start with the first of these commutators.

Keeping in mind that  $\hat{\xi}_K$ ,  $\hat{\zeta}_K$ , and  $\hat{E}_K^{\text{in}}$  all commute with each other at all times

(for fixed  $K$ ), we have

$$\begin{aligned}
[\hat{E}_A^{\text{out}}(t), \hat{E}_B^{\text{out}}(s)] &= e^{i\hat{\xi}_A(t)} e^{i\hat{\zeta}_A(t)} \hat{E}_A^{\text{in}}(t) \times e^{i\hat{\xi}_B(s)} e^{i\hat{\zeta}_B(s)} \hat{E}_B^{\text{in}}(s) \\
&\quad - e^{i\hat{\xi}_B(s)} e^{i\hat{\zeta}_B(s)} \hat{E}_B^{\text{in}}(s) \times e^{i\hat{\xi}_A(t)} e^{i\hat{\zeta}_A(t)} \hat{E}_A^{\text{in}}(t) \\
&= e^{i\hat{\xi}_A(t)} e^{i\hat{\xi}_B(s)} \left( e^{i\hat{\zeta}_A(t)} \hat{E}_A^{\text{in}}(t) \hat{E}_B^{\text{in}}(s) e^{i\hat{\zeta}_B(s)} \right) \\
&\quad - e^{i\hat{\xi}_B(s)} e^{i\hat{\xi}_A(t)} \left( e^{i\hat{\zeta}_B(s)} \hat{E}_A^{\text{in}}(t) \hat{E}_B^{\text{in}}(s) e^{i\hat{\zeta}_A(t)} \right). \tag{A.30}
\end{aligned}$$

Note that  $\hat{\zeta}_L$  and  $\hat{E}_K^{\text{in}}$  do not commute when  $L \neq K$ , and  $\hat{\xi}_A$  and  $\hat{\xi}_B$  don't commute with each other, so we cannot continue merely rearranging terms. Instead, we must proceed more cleverly. By applying the Baker–Campbell–Hausdorff (BCH) lemma we have

$$\begin{aligned}
[\hat{E}_A^{\text{out}}(t), \hat{E}_B^{\text{out}}(s)] &= e^{i\hat{\xi}_A(t)} e^{i\hat{\xi}_B(s)} \left( e^{i\hat{\zeta}_A(t)} \hat{E}_A^{\text{in}}(t) \hat{E}_B^{\text{in}}(s) e^{i\hat{\zeta}_B(s)} \right) \\
&\quad - e^{-[i\hat{\xi}_A(t), i\hat{\xi}_B(s)]} e^{i\hat{\xi}_A(t)} e^{i\hat{\xi}_B(s)} \left( e^{i\hat{\zeta}_B(s)} \hat{E}_A^{\text{in}}(t) \hat{E}_B^{\text{in}}(s) e^{i\hat{\zeta}_A(t)} \right) \\
&= e^{i\hat{\xi}_A(t)} e^{i\hat{\xi}_B(s)} \left( e^{i\hat{\zeta}_A(t)} \hat{E}_A^{\text{in}}(t) \hat{E}_B^{\text{in}}(s) e^{i\hat{\zeta}_B(s)} \right) \\
&\quad - e^{[\hat{\xi}_A(t), \hat{\xi}_B(s)]} e^{i\hat{\xi}_A(t)} e^{i\hat{\xi}_B(s)} \left( e^{i\hat{\zeta}_B(s)} \hat{E}_A^{\text{in}}(t) \hat{E}_B^{\text{in}}(s) e^{i\hat{\zeta}_A(t)} \right). \tag{A.31}
\end{aligned}$$

After a precognizant introduction of terms that equal the identity we have

$$\begin{aligned}
[\hat{E}_A^{\text{out}}(t), \hat{E}_B^{\text{out}}(s)] &= e^{i\hat{\xi}_A(t)} e^{i\hat{\xi}_B(s)} \left( e^{i\hat{\zeta}_A(t)} \hat{E}_A^{\text{in}}(t) \hat{E}_B^{\text{in}}(s) e^{i\hat{\zeta}_B(s)} \right) \\
&\quad - e^{[\hat{\xi}_A(t), \hat{\xi}_B(s)]} e^{i\hat{\xi}_A(t)} e^{i\hat{\xi}_B(s)} \\
&\quad \left( e^{i\hat{\zeta}_B(s)} \hat{E}_A^{\text{in}}(t) \left[ e^{-i\hat{\zeta}_B(s)} e^{i\hat{\zeta}_B(s)} \right] \left[ e^{i\hat{\zeta}_A(t)} e^{-i\hat{\zeta}_A(t)} \right] \hat{E}_B^{\text{in}}(s) e^{i\hat{\zeta}_A(t)} \right). \tag{A.32}
\end{aligned}$$

Now, some minor regrouping and rearrangement of commuting terms leaves us with

$$\begin{aligned}
[\hat{E}_A^{\text{out}}(t), \hat{E}_B^{\text{out}}(s)] &= e^{i\hat{\xi}_A(t)} e^{i\hat{\xi}_B(s)} \left( e^{i\hat{\zeta}_A(t)} \hat{E}_A^{\text{in}}(t) \hat{E}_B^{\text{in}}(s) e^{i\hat{\zeta}_B(s)} \right) \\
&\quad - e^{[\hat{\xi}_A(t), \hat{\xi}_B(s)]} e^{i\hat{\xi}_A(t)} e^{i\hat{\xi}_B(s)} \\
&\quad \left( e^{i\hat{\zeta}_A(t)} \left[ e^{i\hat{\zeta}_B(s)} \hat{E}_A^{\text{in}}(t) e^{-i\hat{\zeta}_B(s)} \right] \left[ e^{-i\hat{\zeta}_A(t)} \hat{E}_B^{\text{in}}(s) e^{i\hat{\zeta}_A(t)} \right] e^{i\hat{\zeta}_B(s)} \right). \tag{A.33}
\end{aligned}$$

From here, we can apply the following form of the BCH lemma,

$$e^{i\hat{G}\lambda} \hat{A} e^{-i\hat{G}\lambda} = \hat{A} + i\lambda[\hat{G}, \hat{A}] + \frac{(i\lambda)^2}{2!}[\hat{G}, [\hat{G}, \hat{A}]] + \frac{(i\lambda)^3}{3!}[\hat{G}, [\hat{G}, [\hat{G}, \hat{A}]]] + \dots, \quad (\text{A.34})$$

to the bracketed terms of Equation (A.33). From

$$\begin{aligned} [\hat{\zeta}_B(s), \hat{E}_A^{\text{in}}(t)] &= \eta \int_0^L dz \int_{-\infty}^{\infty} dt' h(s-t') [\hat{I}_A(t' - (2z-L)/v), \hat{E}_A^{\text{in}}(t)] \\ &= -\eta \int_0^L dz \int_{-\infty}^{\infty} dt' h(s-t') \delta(t - (t' - (2z-L)/v)) \hat{E}_A^{\text{in}}(t' - (2z-L)/v) \\ &= \left( -\eta \int_0^L dz h(s-t - (2z-L)/v) \right) \hat{E}_A^{\text{in}}(t) \end{aligned} \quad (\text{A.35})$$

we have

$$\begin{aligned} e^{i\hat{\zeta}_B(s)} \hat{E}_A^{\text{in}}(t) e^{-i\hat{\zeta}_B(s)} &= \hat{E}_A^{\text{in}}(t) \\ &\quad + \left( -i\eta \int_0^L dz h(s-t - (2z-L)/v) \right) \hat{E}_A^{\text{in}}(t) \\ &\quad + \frac{\left( -i\eta \int_0^L dz h(s-t - (2z-L)/v) \right)^2}{2!} \hat{E}_A^{\text{in}}(t) + \dots \\ &= e^{-i\eta \int_0^L dz h(s-t-(2z-L)/v)} \hat{E}_A^{\text{in}}(t). \end{aligned} \quad (\text{A.36})$$

Similarly,

$$e^{-i\hat{\zeta}_A(t)} \hat{E}_B^{\text{in}}(s) e^{i\hat{\zeta}_A(t)} = e^{i\eta \int_0^L dz h(t-s+(2z-L)/v)} \hat{E}_B^{\text{in}}(s). \quad (\text{A.37})$$

So, we now have

$$\begin{aligned} [\hat{E}_A^{\text{out}}(t), \hat{E}_B^{\text{out}}(s)] &= e^{i\hat{\zeta}_A(t)} e^{i\hat{\zeta}_B(s)} \left( e^{i\hat{\zeta}_A(t)} \hat{E}_A^{\text{in}}(t) \hat{E}_B^{\text{in}}(s) e^{i\hat{\zeta}_B(s)} \right) \\ &\quad - e^{[\hat{\zeta}_A(t), \hat{\zeta}_B(s)]} e^{i\hat{\zeta}_A(t)} e^{i\hat{\zeta}_B(s)} \left( e^{i\hat{\zeta}_A(t)} \hat{E}_A^{\text{in}}(t) \hat{E}_B^{\text{in}}(s) e^{i\hat{\zeta}_B(s)} \right) \\ &\quad e^{-i\eta \int_0^L dz h(s-t-(2z-L)/v) - h(t-s+(2z-L)/v)}. \end{aligned} \quad (\text{A.38})$$

Finally, making use of the commutator relation for  $\hat{\xi}_A$  and  $\hat{\xi}_B$ , we can see that

$$[\hat{E}_A^{\text{out}}(t), \hat{E}_B^{\text{out}}(s)] = 0. \quad (\text{A.39})$$

The argument for  $[\hat{E}_A^{\text{out}}(t), \hat{E}_B^{\text{out}\dagger}(s)] = 0$  is essentially the same, with some minor differences in signs throughout. With these commutators worked out, it is now clear that Equations (A.17), (A.18), (A.20), and (A.29) describe a consistent continuous-time theory for quantum XPM with counter-propagating pulses.

### A.3 Conditions for a Uniform Phase Shift

As in the co-propagating case, we must now analyze under what conditions a uniform phase shift is attainable, as necessary for building a CPHASE gate. Owing to the close similarities between the co-propagating and counter-propagating theories, the derivations are very similar, and what follows should feel essentially the same as Section 2.2. As before, we take the computational basis state  $|0\rangle$  to be the vacuum state, and we take the computational basis state  $|1\rangle$  to be given by

$$|1\rangle = \int_{-\infty}^{\infty} dt \, \psi(t) |t\rangle. \quad (\text{A.40})$$

Ignoring the phase noise for the time being, the phase shifts induced on each mode by the presence of a single-photon pulse in the other mode are found by taking the partial trace of the phase-shift operator for the mode with respect to the other mode, as follows:

$${}_B\langle 1 | e^{i\hat{\zeta}_A(t)} | 1 \rangle_B = \int ds \, e^{in \int_0^L dz \, h(t-s+(2z-L)/v)} |\psi(s)|^2, \quad (\text{A.41a})$$

$${}_A\langle 1 | e^{i\hat{\zeta}_B(t)} | 1 \rangle_A = \int ds \, e^{in \int_0^L dz \, h(t-s-(2z-L)/v)} |\psi(s)|^2, \quad (\text{A.41b})$$

where a step or two have been omitted. From this, it is clear that a sufficient condition for a uniform phase shift is that the response-function integrals encapsulate the entirety of the response function for all times  $t$  and  $s$  for which  $\psi(t)$  and  $\psi(s)$

are non-zero. So, take  $h$  to be non-zero only over the interval  $[0, t_h]$ , ensuring the response is causal, and take  $\psi$  to be non-zero only over the interval  $[-t_\psi/2, t_\psi/2]$ , so that  $t_\psi$  is the pulse width. While these support conditions may not be able to be met exactly, we can at least take  $t_h$  and  $t_\psi$  to represent the nominal durations over which each function is significantly different from zero. Extracting the response-function integrals, and making a small change of variables, the quantities of interest are

$$\phi_A(t, s) = \eta \frac{v}{2} \int_{-L/v}^{L/v} dz' h(t - s + z'), \quad (\text{A.42a})$$

$$\phi_B(t, s) = \eta \frac{v}{2} \int_{-L/v}^{L/v} dz' h(t - s - z'). \quad (\text{A.42b})$$

For the response-function integrals to encapsulate the entirety of the response, it is clear that the following inequalities must hold:

$$\max_{t, s \in \left[-\frac{t_\psi}{2}, \frac{t_\psi}{2}\right]} \min_{z' \in \left[-\frac{L}{v}, \frac{L}{v}\right]} \{t - s + z'\} \leq 0, \quad (\text{A.43a})$$

$$\min_{t, s \in \left[-\frac{t_\psi}{2}, \frac{t_\psi}{2}\right]} \max_{z' \in \left[-\frac{L}{v}, \frac{L}{v}\right]} \{t - s + z'\} \geq t_h, \quad (\text{A.43b})$$

$$\max_{t, s \in \left[-\frac{t_\psi}{2}, \frac{t_\psi}{2}\right]} \min_{z' \in \left[-\frac{L}{v}, \frac{L}{v}\right]} \{t - s - z'\} \leq 0, \quad (\text{A.43c})$$

$$\min_{t, s \in \left[-\frac{t_\psi}{2}, \frac{t_\psi}{2}\right]} \max_{z' \in \left[-\frac{L}{v}, \frac{L}{v}\right]} \{t - s - z'\} \geq t_h. \quad (\text{A.43d})$$

Plugging in the appropriate maximum and minimum values of  $t$ ,  $s$ , and  $z'$  and removing redundancies results in the following single sufficient condition:

$$\frac{L}{v} \geq t_h + t_\psi. \quad (\text{A.44})$$

Our symmetry assumptions about the pulses already enforces the condition that, physically, both pulses enter the material at the same time (at opposite ends of the nonlinear material). Now, Equation (A.44) mandates that the material be long enough to house both pulses in their entirety at the same time, in addition to the response tails they drag behind them. (In the fast-response case, the condition reduces

to  $L \geq vt_\psi$ , i.e. that the material be long enough to contain the pulses.) Taking the response function to be normalized, we see that the magnitude of the phase shift is given by

$$\phi = \eta v/2. \quad (\text{A.45})$$

Note that, as in the co-propagating case (Equation (2.19))

$$\eta L = 2\phi(t_\psi + t_h). \quad (\text{A.46})$$

So, the results presented in Chapter 3 apply equally well to the case of counter-propagating pulses.

Comparing Equations (2.18) and (A.45) reveals why the co-propagating case gives a much larger nonlinear phase shift, from the same material, than does the counter-propagating case. Fixing  $\eta$  we have

$$\frac{\phi_{\text{counter}}}{\phi_{\text{co}}} = \frac{v}{2u} = \frac{v}{2} \left( \frac{1}{v_A} - \frac{1}{v_B} \right) = \frac{v(v_B - v_A)}{2v_A v_B} \ll 1. \quad (\text{A.47})$$

The final inequality follows from the fact that, in practice,  $v$ ,  $v_A$ , and  $v_B$  will all be relatively close to each other.



# Bibliography

- [1] Chris Chudzicki. Research notes: XPM with differing group velocities. *Internal memo, MIT Research Lab of Electronics*, Aug 2012.
- [2] Peter Shor. Polynomial-time algorithms for prime factorization and discrete logarithms on a quantum computer. *SIAM Review*, 41(2):303–332, 1999. doi: 10.1137/S0036144598347011. URL <http://epubs.siam.org/doi/abs/10.1137/S0036144598347011>.
- [3] Lov K. Grover. A fast quantum mechanical algorithm for database search, 1996.
- [4] Aram W. Harrow, Avinatan Hassidim, and Seth Lloyd. Quantum algorithm for linear systems of equations. *Phys. Rev. Lett.*, 103:150502, Oct 2009. doi: 10.1103/PhysRevLett.103.150502. URL <http://link.aps.org/doi/10.1103/PhysRevLett.103.150502>.
- [5] Seth Lloyd. Universal quantum simulators. *Science*, 273(5278):1073–1078, 1996. doi: 10.1126/science.273.5278.1073. URL <http://www.sciencemag.org/content/273/5278/1073.abstract>.
- [6] Emanuel Knill, Raymond Laflamme, and Gerald J. Milburn. A scheme for efficient quantum computation with linear optics. *Nature*, 409(6816):46–52, Jan 2001. ISSN 0028-0836. doi: 10.1038/35051009. URL <http://dx.doi.org/10.1038/35051009>.
- [7] Isaac L. Chuang and Yoshihisa Yamamoto. Simple quantum computer. *Phys. Rev. A*, 52:3489–3496, Nov 1995. doi: 10.1103/PhysRevA.52.3489. URL <http://link.aps.org/doi/10.1103/PhysRevA.52.3489>.
- [8] Jeffrey H. Shapiro and Roy S. Bondurant. Qubit degradation due to cross-phase-modulation photon-number measurement. *Phys. Rev. A*, 73:022301, Feb 2006. doi: 10.1103/PhysRevA.73.022301. URL <http://link.aps.org/doi/10.1103/PhysRevA.73.022301>.
- [9] Luc Boivin, Frans X. Kärtner, and Herman A. Haus. Analytical solution to the quantum field theory of self-phase modulation with a finite response time. *Phys. Rev. Lett.*, 73:240–243, Jul 1994. doi: 10.1103/PhysRevLett.73.240. URL <http://link.aps.org/doi/10.1103/PhysRevLett.73.240>.

- [10] Paul L Voss and Prem Kumar. Raman-effect induced noise limits on  $\chi^{(3)}$  parametric amplifiers and wavelength converters. *Journal of Optics B: Quantum and Semiclassical Optics*, 6(8):S762, 2004. URL <http://stacks.iop.org/1464-4266/6/i=8/a=021>.
- [11] Jeffrey H. Shapiro and Asif Shakeel. Optimizing homodyne detection of quadrature-noise squeezing by local-oscillator selection. *J. Opt. Soc. Am. B*, 14(2):232–249, Feb 1997. doi: 10.1364/JOSAB.14.000232. URL <http://josab.osa.org/abstract.cfm?URI=josab-14-2-232>.
- [12] Jeffrey H. Shapiro. Single-photon kerr nonlinearities do not help quantum computation. *Phys. Rev. A*, 73:062305, Jun 2006. doi: 10.1103/PhysRevA.73.062305. URL <http://link.aps.org/doi/10.1103/PhysRevA.73.062305>.
- [13] Marius Mařalas and Michael Fleischhauer. Scattering of dark-state polaritons in optical lattices and quantum phase gate for photons. *Phys. Rev. A*, 69:061801, Jun 2004. doi: 10.1103/PhysRevA.69.061801. URL <http://link.aps.org/doi/10.1103/PhysRevA.69.061801>.
- [14] Inbal Friedler, Gershon Kurizki, and David Petrosyan. Deterministic quantum logic with photons via optically induced photonic band gaps. *Phys. Rev. A*, 71:023803, Feb 2005. doi: 10.1103/PhysRevA.71.023803. URL <http://link.aps.org/doi/10.1103/PhysRevA.71.023803>.
- [15] Yong-Fan Chen, Chang-Yi Wang, Shih-Hao Wang, and It'e A. Yu. Low-light-level cross-phase-modulation based on stored light pulses. *Phys. Rev. Lett.*, 96:043603, Feb 2006. doi: 10.1103/PhysRevLett.96.043603. URL <http://link.aps.org/doi/10.1103/PhysRevLett.96.043603>.
- [16] Karl-Peter Marzlin, Zeng-Bin Wang, Sergey A. Moiseev, and Barry C. Sanders. Uniform cross-phase modulation for nonclassical radiation pulses. *J. Opt. Soc. Am. B*, 27(6):A36–A45, Jun 2010. doi: 10.1364/JOSAB.27.000A36. URL <http://josab.osa.org/abstract.cfm?URI=josab-27-6-A36>.
- [17] R. H. Stolen, J. P. Gordon, W. J. Tomlinson, and H. A. Haus. Raman response function of silica-core fibers. *J. Opt. Soc. Am. B*, 6(6):1159–1166, Jun 1989. doi: 10.1364/JOSAB.6.001159. URL <http://josab.osa.org/abstract.cfm?URI=josab-6-6-1159>.
- [18] Christopher Chudzicki, Isaac L. Chuang, and Jeffrey H. Shapiro. Deterministic and cascable conditional phase gate for photonic qubits. *Phys. Rev. A*, 87:042325, Apr 2013. doi: 10.1103/PhysRevA.87.042325. URL <http://link.aps.org/doi/10.1103/PhysRevA.87.042325>.
- [19] Yu-Zhu Sun, Yu-Ping Huang, and Prem Kumar. Photonic nonlinearities via quantum zeno blockade. *Phys. Rev. Lett.*, 110:223901, May 2013. doi: 10.1103/PhysRevLett.110.223901. URL <http://link.aps.org/doi/10.1103/PhysRevLett.110.223901>.